



Review article

# The Inner Phase of Molecular Container Compounds as a Novel Reaction Environment \*

RALF WARMUTH

Department of Chemistry, Kansas State University, Manhattan, KS 66506-3701, U.S.A.

(Received: 2 December 1998; in final form: 11 January 1999)

**Abstract.** The conceptual idea of molecular container compounds and their synthesis has opened an entirely new and very interesting research field: the chemistry of and within molecular container compounds and their complexes. Molecular containers have inner phases just large enough to accommodate a single guest molecule. Beginning with Donald J. Cram's first synthesis of a carcerand, which permanently entrapped a single guest molecule, many other containers such as hemicarcerands, molecular lantern, self-assembled capsules and fullerenes have been synthesized and studied. Not only is the design and development of new container compounds an ongoing challenge for organic chemists, but also the systematic investigation of chemical reactions within their inner phases. The results of a large variety of inner phase reactions spanning acid-base, reduction, oxidation, nucleophilic substitution, addition, thermal, photochemical and pericyclic reactions have provided us with more insight into the relationship between bulk phase and inner phase reactants and the mechanism of the transfer of electrons and photons through the insulating shell of a container molecule. They have also led to very spectacular applications of molecular container compounds such as the stabilization of reactive intermediates by incarceration. These highlights of inner phase chemistry and the current efforts and successes towards using molecular containers as catalytic reaction vessels are presented and discussed.

**Key words:** molecular container compound, hemicarcerand, fullerene, self-assembled capsules, reaction bowl, molecular lantern, encapsulation, inner phase, reactive intermediate, excited state, *o*-benzyne, photo-electron-transfer, electron-transfer, proton-transfer, catalysis, Diels-Alder reaction, nucleophilic substitution, isotopic exchange.

## 1. Introduction

If two bowl-shaped molecules are connected rim-to-rim, a closed-shell spherical molecule results which is wrapped around an inner space large enough to occupy an organic guest molecule. This was Donald J. Cram's conceptual idea that led him to design and synthesize the first molecular container compound which he called a carcerand [1]. The name carcerand is derived from *ligand* and from the Latin word *carcer*, meaning prison, which truly suits this new class of compounds.

---

\* Dedicated to Professor Donald J. Cram on the occasion of his 80th birthday.

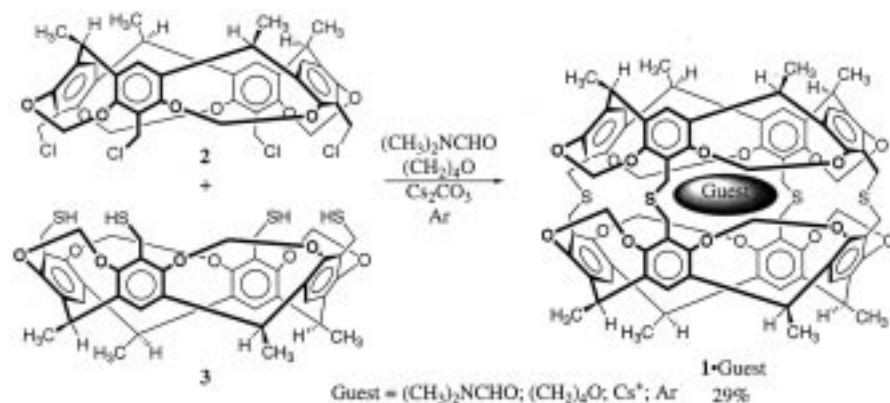


Chart 1.

Carcerands such as **1** differ from other organic molecules in that they have two distinct, non-connected surfaces. Its outer surface is exposed to the bulk phase and its inner surface sets the boundaries for its inner cavity. Indeed, a single organic molecule can be incarcerated in these cavities. The guest is held inside by constrictive binding, a new binding phenomenon which results if the portals are too narrow, preventing guest escape. Isolated from the bulk phase, the guest can freely rotate and translate inside its molecular prison [2]. Cram coined the name “inner phase” for the interior of a container compound since the properties of an incarcerated guest molecule are different from those in the bulk phase.

In 1985, Cram and coworkers reported the first successful carceplex synthesis [3]. When equimolar amounts of the two cavitands **2** and **3** were treated with  $\text{Cs}_2\text{CO}_3$  in a mixture of dimethylformamide (DMF) and tetrahydrofuran (THF) under high dilution conditions, a mixture of different carceplexes **1·Guest** were obtained as insoluble material in 29% yield.

Despite the unexpected insolubility of these carceplexes which prevented the application of solution NMR techniques for their structural analysis, their exact composition could be determined via elemental analysis, IR and FAB-MS in combination with chemical tests. During its formation, **1** essentially incarcerated every component present in the reaction mixture that can be accommodated in its inner cavity in Corey–Pauling–Koltun (CPK) space filling models. The FAB-MS showed signals for **1·Guest**, with the guests argon, DMF, THF,  $\text{H}_2\text{O}$ ,  $\text{Cs}^+$ , and also  $\text{ClCF}_2\text{CF}_2\text{Cl}$ , if the shell-closure reaction was performed in the presence of  $\text{ClCF}_2\text{CF}_2\text{Cl}$  (Freon). If in the latter case, the carceplex mixture was degraded with refluxing trifluoroacetic acid, free  $\text{ClCF}_2\text{CF}_2\text{Cl}$  could be detected by GC-MS. Variation of the appendent substituents allowed the preparation of soluble carceplexes **4·Guest** and **5·Guest** in subsequent studies [4].

Since the first carceplex synthesis, a large variety of (hemi)carcerands with different shapes and sizes of their inner cavities have been prepared in the laboratories of D. J. Cram and others by connecting two cavitands together with four

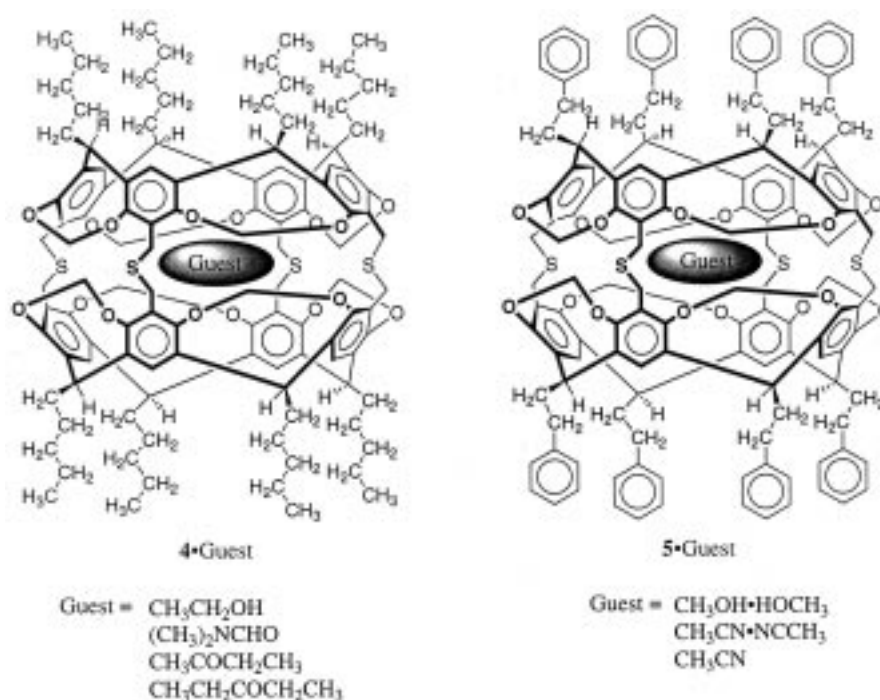


Chart 2.

appropriate linkers [5–10] and their binding properties have been studied. These (hemi)carcerands have cavities suitable for the incarceration of guests of a wide range of sizes and shapes from small molecules such as  $\text{N}_2$ ,  $\text{O}_2$ , or  $\text{Xe}$  [5d] to molecules as large as  $\text{C}_{60}$  which itself is a container [5j]. A very important break through has been the recent synthesis of the first water-soluble hemicarcerand by Yoon and Cram which will direct this field into a new dimension [10].

The novelty of the (hemi)carcerand structures have lured molecular container chemists to study their properties and the properties of their trapped guests. For example, the mechanism of their template assisted formation which leads in one case to exceptionally high yields of 87% for a reaction that involves the collection of seven components and the formation of eight covalent bonds [11]; the relationship between size, shape, and electronic nature of the inner phase and their binding properties [1b–c, 2, 5–8, 10]; the mystery around the mechanism of guest entrance or exit at high temperature in complexes, whose guest freely rotates and which are almost infinitely stable at room temperature [12, 7b]. Furthermore, there are many interesting questions related to the guest reactivity: Could one conduct reactions inside these reaction vessels and how would those reactions differ from their bulk phase counterparts? How do small reactants such as protons, electrons or photons pass through the host skeleton in order to reach the incarcerated guest? Can we even generate and protect highly delicate molecules inside the inner phase and prevent

their self-destruction via dimerization or the reaction with bulk phase reactants that are too large to pass through the protective host skin? Is catalysis possible in such novel reaction chambers?

In the following, I will summarize all recent efforts to answer the latter questions regarding inner phase reactions and the stabilization of reaction intermediates inside molecular containers such as hemicarcerands, fullerenes, molecular lanterns and hydrogen-bonded self-assembled capsules ('soft-balls'). This will provide the reader with an overview of inner phase chemistry starting from the discovery of molecular containers by Donald. J. Cram until now, and an outlook on how this exciting research field might develop.

## 2. Inner Phase Reactions

Reactions in inner phases are at the interface between solution phase and bulk phase reactions. On one hand, one can treat a molecular container as a novel reaction flask and the inner phase and its incarcerated guest as a single molecule gas. In such a single molecule gas, the mobility of the reactant is more restricted by the host compared to a macroscopic gas. However, we can also regard inner phase reactions as similar to solution phase reactions in which reactants and encounter complexes are surrounded by solvent cages. Areas of the rigid inner host surface function as such a solvent cage which has to stabilize the inner phase reaction transition states. It is clear that such inner phase reactions will considerably differ from their analogous solution or gas phase counterparts. Conceptually, we can divide inner phase reactions into four categories:

1. Intermolecular inner phase reactions.
2. Intramolecular inner phase reactions.
3. Mother molecule–daughter molecule inner phase reactions.
4. Inermolecular inner phase reactions.

In intermolecular inner phase reactions, the incarcerated guest reacts with a bulk phase reactant. This may require the full incarceration of both reactants or the partial passage of the bulk phase reactant through one of the openings in the host shell. In most observed bimolecular inner phase reactions carried out inside hemicarcerands, it is difficult to discriminate between both models. Many different intermolecular reactions, which will be summarized in Sections 3 and 5, have been carried out with sometimes very surprising outcomes and have led to the discovery of the first real catalytic reaction chamber.

Intramolecular inner phase reactions are triggered by an external stimulus (e.g., light or heat) that causes the rearrangement of the incarcerated guest or its cleavage into two or more fragments which subsequently might exit the inner phase. Such reactions which have led to the generation and stabilization of incarcerated reactive intermediates will be discussed in Section 3.

Two further new inner phase reaction types have been introduced recently. In Okazaki's mother molecule–daughter molecule-reactions, an external stimulus

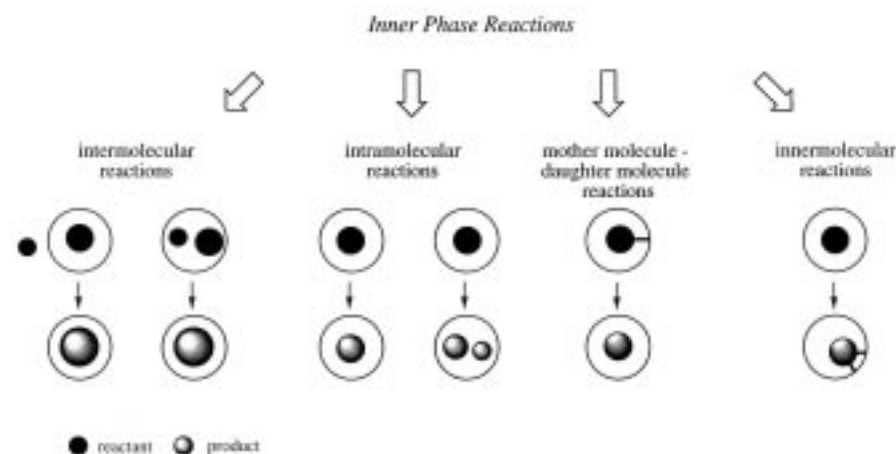


Figure 1. The graphic shows different types of inner phase reactions which have been observed.

leads to the release of a guest (daughter) which was covalently linked to the inner surface of the surrounding host (mother) to form a new mother molecule–daughter molecule complex. Innermolecular reactions are the exact opposite. The incarcerated guest reacts with the inner surface of the surrounding molecular container leading to a covalent adduct. The latter two reaction types are particularly interesting. The mother molecule–daughter molecule complex formation allows the generation of an encapsulated reactive intermediate or of an endohedral-fixed reactive functionality, which both are protected by the surrounding capsule shell. Recent application of this principle will be discussed in Section 6. Innermolecular reactions are interesting since these reactions take place at the concave inner surface of one reactant (the host), which is rather uncommon. Such type of reactions will be discussed in Sections 3 and 6.

### 3. Hemarcerands as Unimolecular Reaction Vessels

#### 3.1. PROTON-TRANSFER REACTIONS

In order to answer the question of whether reactions between incarcerated guest molecules and bulk phase reactants through the shell of the surrounding host are possible, proton transfer reactions come immediately to mind due to the small size of the proton. Through-shell protonations also provide insight into the effect of incarceration on the acidity and basicity of guests compared to their bulk phase counterparts. Cram and coworkers addressed these questions by studying through-shell proton transfer reactions of incarcerated amines **6**·pyridine, **6**·(CH<sub>3</sub>CH<sub>2</sub>)<sub>2</sub>NH and **6**·CH<sub>3</sub>(CH<sub>2</sub>)<sub>3</sub>NH<sub>2</sub> [5d].

Despite the fact that the chosen hemarcerand **6** provides large enough holes in its shell for the free passage of H<sup>+</sup>, any attempt to protonate incarcerated pyridine

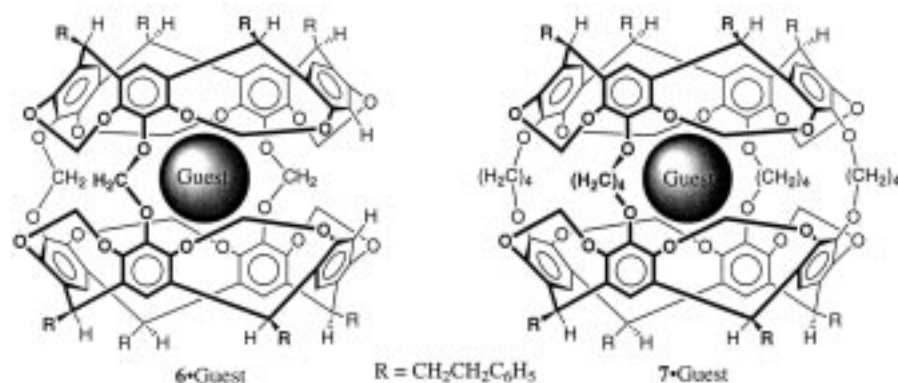


Chart 3.

**6**-pyridine with bulk phase  $\text{CF}_3\text{COOD}$  in  $\text{CDCl}_3$  failed. Under the same conditions, free pyridine was quantitatively protonated. As expected for a hydrophobic inner phase, incarcerated pyridine is much less basic than freely dissolved pyridine. Cram suggested that this reduced basicity is possibly due to the ineffective solvation of the pyridinium ion by the rigid host, the inability to form a contact ion pair in the inner phase, and the larger size of the pyridinium ion compared to the pyridine. An inaccessibility of the unshared electron pair of incarcerated, freely rotating, pyridine would be a possible explanation, but seems very unlikely.

Through-shell proton transfer was possible with  $\mathbf{6} \cdot (\text{CH}_3\text{CH}_2)_2\text{NH}$  accompanied by the instantaneous decomplexation of  $\mathbf{6} \cdot (\text{CH}_3\text{CH}_2)_2\text{ND}_2^+$ . The ability to protonate  $\mathbf{6} \cdot (\text{CH}_3\text{CH}_2)_2\text{NH}$  with  $\text{CF}_3\text{COOD}$  in  $\text{CDCl}_3$  results from the location of the nitrogen of  $(\text{CH}_3\text{CH}_2)_2\text{NH}$  in the equatorial region close to the portals. After protonation, the counterion pulls the guest out of the inner phase. If 10 eq. of  $\text{CF}_3\text{COOD}$  was added to the incarcerated isomeric  $\mathbf{6} \cdot \text{CH}_3(\text{CH}_2)_3\text{NH}_2$ , a 2:1 mixture of  $\mathbf{6} \cdot \text{CH}_3(\text{CH}_2)_3\text{ND}_3^+$  and  $\mathbf{6} \cdot \text{CH}_3(\text{CH}_2)_3\text{NH}_2$  was detected by  $^1\text{H-NMR}$  spectroscopy. This ratio remained constant over time although decomplexation slowly continued at 22 °C with a rate half-life time of 22 min to give free **6** and  $\text{CH}_3(\text{CH}_2)_3\text{ND}_3^+ \cdot ^-\text{O}_2\text{CCF}_3$ . Complete protonation of  $\mathbf{6} \cdot \text{CH}_3(\text{CH}_2)_3\text{NH}_2$  was only possible with 100 eq. of  $\text{CF}_3\text{COOD}$ . However, the addition of a large excess of the weaker acid  $\text{CD}_3\text{COOD}$  resulted only in a H/D exchange of the amine protons. These results show that the acidity of incarcerated n-butylamine is comparable to the acidity of trifluoroacetic acid in  $\text{CDCl}_3$ . The strong upfield-shifted amine protons of  $\mathbf{6} \cdot \text{CH}_3(\text{CH}_2)_3\text{NH}_2$  ( $\Delta\delta$  3.18 ppm) imply a guest alignment along the polar axis of **6**. Model examinations suggest that in this orientation, the through-shell protonation occurs most likely through the holes in the polar caps of **6**.

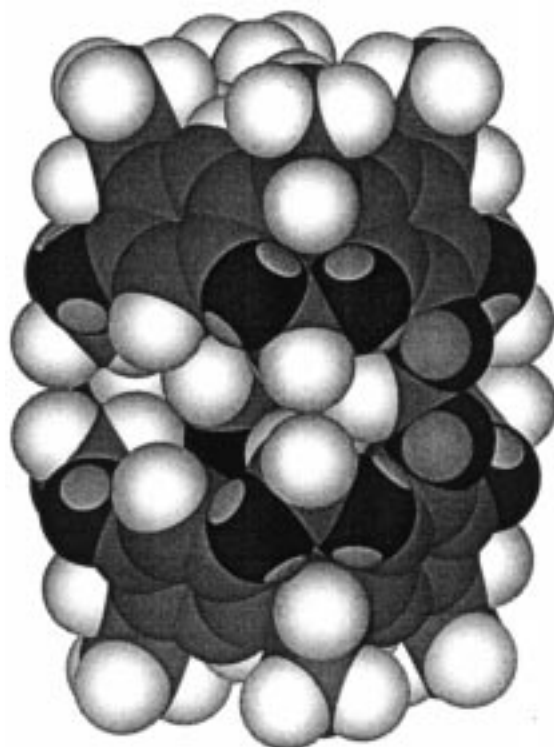


Figure 2. Space-filling model of 6-pyridine showing the exposed nitrogen of the pyridine guest. The pendent groups  $R = \text{CH}_2\text{CH}_2\text{C}_6\text{H}_5$  of **6** are substituted for  $\text{CH}_3$  groups.

### 3.2. ELECTRON-TRANSFER REACTIONS

Electron transfer (ET) plays an important role in many organic reactions and is heavily studied experimentally and theoretically. Although ET processes are most efficient upon contact donor acceptor complexes, it does not necessarily require the direct contact between donor and acceptor. In this case ET would be nonadiabatic. Due to the small size of the electron, ET reactions are well suited to be studied between an incarcerated guest and a bulk phase reducing or oxidizing agent. An oxidation-reduction cycle for the four hydroquinones **8–11** could be carried out in the inner phase of **7** [13].

Oxidation with  $\text{Ce}(\text{NH}_4)_2(\text{NO}_2)_6$ -silica gel- $\text{CCl}_4$  or  $\text{Tl}(\text{O}_2\text{CCF}_3)_3$ - $\text{CCl}_4$  led to the parent incarcerated quinones **12–15** in essentially quantitative yields. Despite their usual instability if in solution, the incarcerated quinones were stable below 100 °C in the absence of light, protected from self-destruction by the surrounding host. The reduction back to the hydroquinones was possible with  $\text{SmI}_2/\text{MeOH}$ . The same reagent reduced incarcerated nitrobenzene **16** to *N*-hydroxyl-aniline **17**. Surprisingly, aniline, which is the product in the liquid phase, is not formed. This latter result, the high yields, and the instability of free *o*-

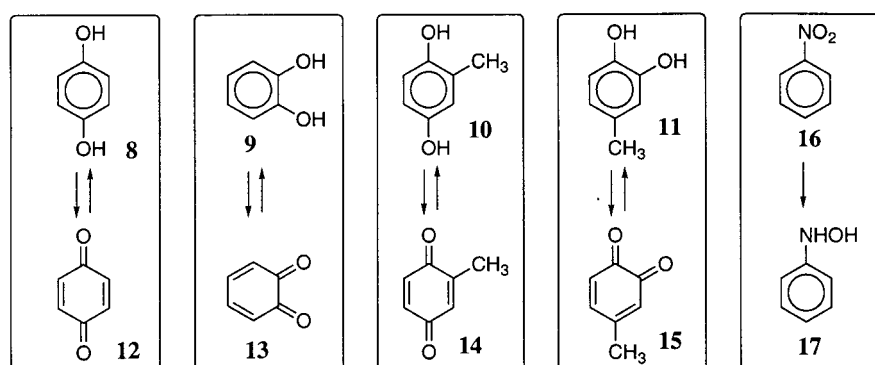


Chart 4.

quinones, suggests that all reduction/oxidation took place in the inner phase, rather than by a dissociation – bulk phase reaction – association mechanism. It also demonstrates that electrons are transferred readily through the host shell in and out of the inner phase. The exact mechanism of the ET and the role of the intervening medium (the host) is not clear yet. To get more insight, Kaifer and coworkers recently compared the electrochemical behavior of free ferrocene with that of incarcerated ferrocene (**18**·ferrocene) [14]. They demonstrated successfully a reversible heterogeneous electron transfer. However, in the inner phase, the ET was strongly hindered kinetically and thermodynamically. A more positive half-way potential for the oxidation, due to the strongly hydrophobic nature of the inner phase, as well as a 10-fold rate retardation was measured. To support their conclusion of an inner phase oxidation/reduction cycle, Kaifer isolated the incarcerated oxidized ferrocene hemicarceplex **18**·ferrocene<sup>+</sup> as a dark blue solid. The NMR spectrum showed large spectral shifts compared to the spectrum of **18**·ferrocene and also strong linebroadening. Both results are consistent with the formation of the paramagnetic guest ferrocene<sup>+</sup>. The blue color and the NMR spectrum persisted at room temperature for several days until **18**·ferrocene<sup>+</sup> slowly reverted back to **18**·ferrocene, revealing that guest dissociation/association can be excluded within the time frame of the electrochemical experiments. Kaifer suggested that the slower ET between the incarcerated ferrocene and the electrode surface could result partially from the higher mass of **18**·ferrocene compared to ferrocene and also from a reduction of the electronic coupling between the ferrocene center and the electrode which is affected by a remarkable increase in distance from 3.5 Å to about 9 Å. Whether the hemicarcerand's aromatic structure may mediate the electron coupling between incarcerated ferrocene and the electrode surface is not clear on the basis of the limited amount of data.



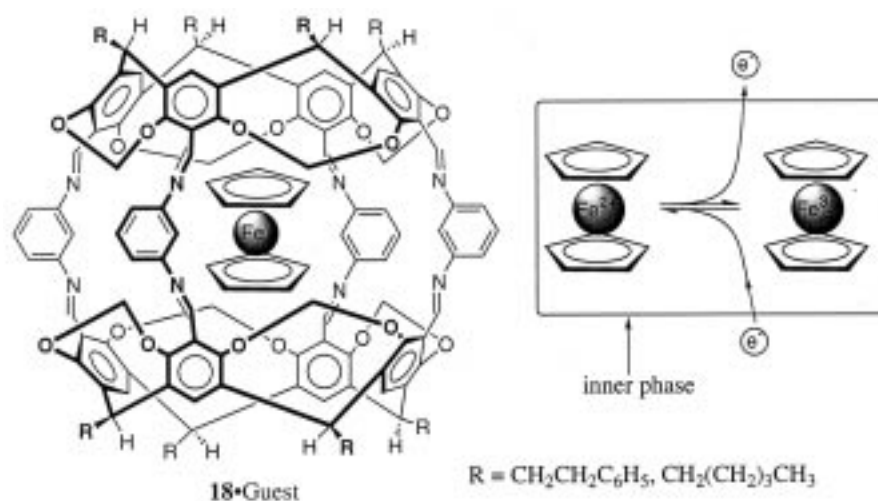


Chart 5.

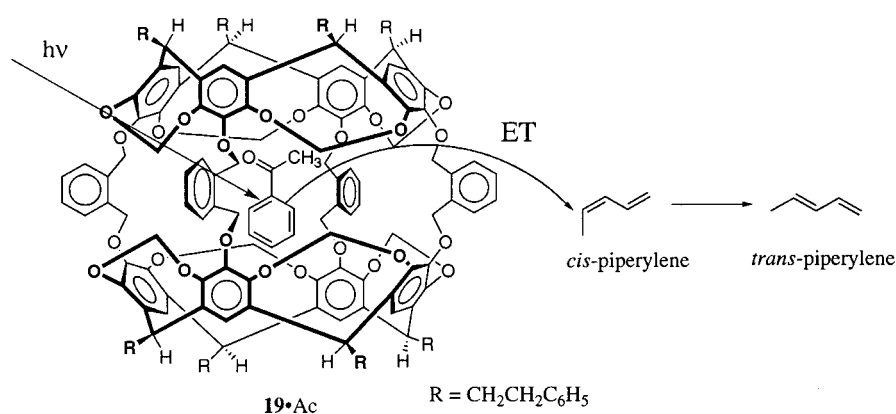


Chart 6.

### 3.3. PHOTO-ELECTRON-TRANSFER AND TRIPLET ENERGY TRANSFER

To get more insight into the mechanism of electron transfers between a donor and an acceptor which are separated by an 'insulating' material, Kurt Deshayes *et al.* started a systematic investigation of triplet energy transfer processes from an incarcerated guest through the surrounding hemicarcerand shell to a bulk phase acceptor [15]. They chose as the incarcerated donor the triplet sensitizer acetophenone (Ac). Acetophenone forms a hemicarceplex with host **19** which is stable at room temperature. Indeed, hemicarceplex **19**·Ac was able to photo-sensitize the isomerization of *cis*-piperylene to *trans*-piperylene, when a solution of *cis*-piperylene and **19**·Ac was irradiated.

Taking into account the different lifetimes of free (240 ns) and incarcerated triplet acetophenone (160 ns), Deshayes *et al.* determined a 2.7-fold slower triplet

&lt;structural formulor of biacetyl&gt;



Scheme 1.

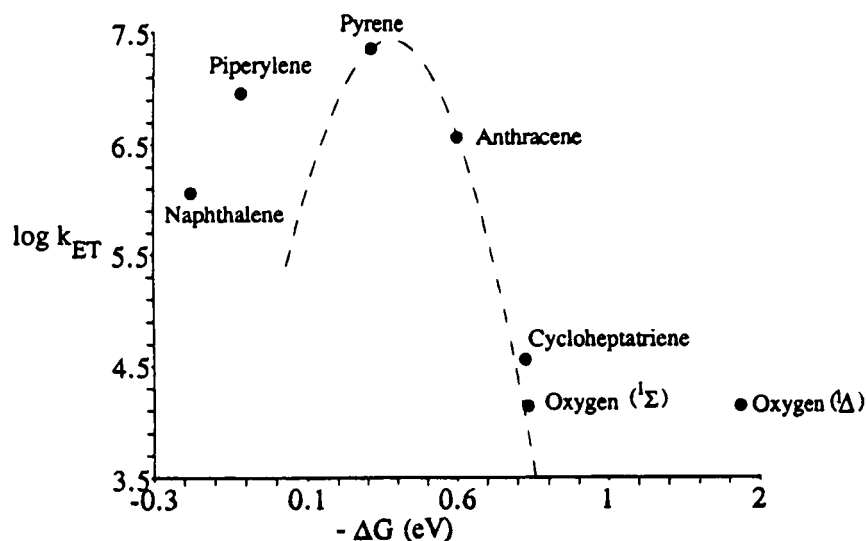


Figure 3. Rates of triplet energy transfer vs.  $-\Delta G$  for **19**·biacetyl and theoretical curve for  $k = A \exp[-(\lambda_s + \Delta G + \lambda_v)^2/4\lambda_s k_B T]$  with  $\lambda_s = 0.2$  eV and  $\lambda_v = 0.2$  eV. Reprinted with permission from *J. Phys. Chem.*, February 1996, **100**, 3305–3307. Copyright 1996 American Chemical Society.

energy transfer rate for **19**·Ac compared to free acetophenone. This corresponds to an almost diffusion controlled rate for **19**·Ac. Deshayes *et al.* concluded that triplet energy is transferred through the shell by an electron exchange mechanism which is believed to require a close contact between donor and acceptor. Since a direct contact is impossible in the present case, sufficient overlap of the HOMO and LUMO of the donor-acceptor pair through the host-shell must exist. This example unambiguously proves the possibility of a pure through-space pathway for a triplet energy transfer. The precise role of the intervening hemicarcerand in such through space energy transfers is not clear based on this study. In an extension of their initial work, Farrán and Deshayes studied the triplet energy transfer between incarcerated biacetyl (Scheme 1) (**19**·biacetyl) and various bulk phase triplet energy acceptors. They found that the hemicarcerand retards the triplet energy transfer in all cases [16].

The hyperbolic relationship between the logarithm of the measured triplet energy transfer rate constant  $k_{ET}$  and the driving force  $\Delta G$  is consistent with a nonadiabatic system that moves into the inverted region at low exothermicity (Figure 3).

The decreased triplet energy transfer rates with **19**-biacetyl suggest a reduced electron-coupling between donor and acceptor as a result of the intervening distance imposed by the hemicarcerand. Consistent with this model is that the measured triplet energy transfer rate constants decrease with increasing thermodynamic driving force, as the Golden Rule predicts for weakly coupled nonadiabatic processes.

Very interesting is the extremely slow triplet energy transfer rate to oxygen with **19**-biacetyl, despite the fact that oxygen is a highly efficient triplet energy quencher. Farrán and Deshayes concluded that when oxygen is prevented from coming into direct contact with the donor, the quenching rate drops off drastically. In an independent investigation using the same donor **19**-biacetyl, Pina *et al.* measured a similar triplet energy transfer rate constant to oxygen [17]. Furthermore, Parola *et al.* independently studied the triplet energy transfer rates with the donors **19**-biacetyl and free biacetyl to various triplet energy quenchers that quench via energy transfer [18]. In addition to the quenchers shown in Figure 3, phenanthrene, 9-fluorenone, benzanthrone and acridine were investigated. The measured triplet energy transfer rates basically coincided with those of Farrán and Deshayes. However, Parola *et al.* concluded that the difference in energy transfer rate constants of free and incarcerated biacetyl is a result of different electronic exchange matrix elements, rather than the different Franck-Condon factors as suggested by Farrán and Deshayes. Parola *et al.* argued that it is very unlikely that the electronic exchange matrix element is constant throughout the series of structurally different triplet quenchers used in both studies. In particular, the large scattering of the data and the poor correlation is likely a consequence of the different sizes of the hydrocarbon quenchers. This results in different donor-acceptor distances and/or orientations leading to different values for the electronic exchange matrix elements. Similar poor correlation and scattering of data was observed in other donor-acceptor pairs covalently connected with a rigid spacer [19]. Hence, Parola *et al.* are rather careful in taking the observed parabolic like relationship as firm evidence for inverted behavior as suggested by Farrán and Deshayes.

Nevertheless, triplet energy transfer reactions between a donor and acceptor which are separated by an insulation barrier are truly novel. The complexity of such systems is enormous as should be obvious from the above discussion. Since our knowledge and understanding about carceplexes and hemicarceplexes is not complete yet, further more detailed studies are required and are already underway in Deshayes' laboratories [20]. We can look with great excitement towards the results of these investigations which will hopefully favor one of these models.

### 3.4. THROUGH-SHELL NUCLEOPHILIC SUBSTITUTIONS AND ISOTOPIC EXCHANGE REACTIONS

Much insight into the relationship between guest reactivity, guest orientation and bulk phase reagent size was provided by the alkylation studies of Kurdistani *et*

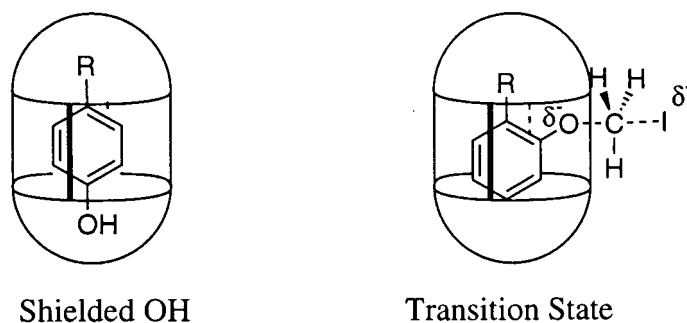


Figure 4. Preferred orientation of *para*-substituted phenols and the linear transition state for the methylation of an incarcerated *ortho*-substituted phenolate in the inner phase of hemicarcerand **7**.

*al.* [7a] These relationships are very characteristic for through-shell reactions. Different phenols were alkylated in the inner phase of **7** [5h]. Two factors determined the observed reactivity: (a) the portal size, and (b) the guest orientation in the inner phase. The ability to methylate the phenolic OH-groups with NaH/MeI in THF can be correlated to the preferred guest orientation in the inner phase relative to an equatorial-located portal. Alkylation of 4-HOC<sub>6</sub>H<sub>4</sub>CH<sub>3</sub> (*p*-cresol) or 4-HOC<sub>6</sub>H<sub>4</sub>OH (*p*-hydroquinone) was impossible. Under the same conditions, 2-HOC<sub>6</sub>H<sub>4</sub>CH<sub>3</sub> (*o*-cresol), 3-HOC<sub>6</sub>H<sub>4</sub>CH<sub>3</sub> (*m*-cresol), and 3-HOC<sub>6</sub>H<sub>4</sub>OH (resorcinol) were quantitatively methylated. 2-HOC<sub>6</sub>H<sub>4</sub>OH (catechol) gave a mixture of mono- and dimethylated carceplexes.

An examination of typical crystal structures of 1,4-disubstituted benzene hemicarceplexes **7**·Guest such as the 1,4-diiodobenzene or the *p*-xylene hemicarceplex [5h], suggests that the OH-group of 4-HOC<sub>6</sub>H<sub>4</sub>CH<sub>3</sub> would be located in a protected polar cap of the host. On the other hand, *ortho*- or *meta*-disubstituted benzene guests have one of the substituents located inside a shielded polar cap of the host, whereas the second substituent is located near an equatorial-located entryway. This suggests that these reactions must occur in the entryways through a linear transition state which is partially 'solvated' by the alkoxy-units that align the host's portals (Figure 4). Since this 'pseudo solvent cage' has limited conformational flexibility, the alkylation with larger alkylating agents failed.

Similarly, no D-for-H exchange of the hydroxyls of **7**·Guest was possible in D<sub>2</sub>O-saturated CDCl<sub>3</sub> when guests were 4-HOC<sub>6</sub>H<sub>4</sub>CH<sub>3</sub>, 2-HOC<sub>6</sub>H<sub>4</sub>OH or 4-HOC<sub>6</sub>H<sub>4</sub>OH. In the presence of the large base diazabicyclo[5.4.0]undec-7-ene (DBU), 4-HOC<sub>6</sub>H<sub>4</sub>OH exchanges its hydroxyl-protons, whereas the more conformationally fixed 4-HOC<sub>6</sub>H<sub>4</sub>CH<sub>3</sub> does not. In THF-NaH at 25 °C followed by D<sub>2</sub>O-quench, the hydroxyl-protons of 2-HOC<sub>6</sub>H<sub>4</sub>OH which are more exposed to the equatorial-located hemicarcerand portals exchange, but the more protected hydroxyl-protons of 4-HOC<sub>6</sub>H<sub>4</sub>OH and 4-HOC<sub>6</sub>H<sub>4</sub>CH<sub>3</sub> do not exchange.

Such steric interactions in the transition state that are serving as selectivity criteria in these inner phase reactions also contribute to the highly structural re-

cognition in enzyme-catalyzed reactions. The understanding of these interactions will give us valuable guidelines for the rational design of novel highly selective catalysts in the future.

### 3.5. PHOTOCHEMICAL GENERATION OF REACTIVE INTERMEDIATES

One of the most ingenious, unparalleled applications of hemicarcerands is the inner phase stabilization of reactive intermediates. The surrounding hemicarcerand serves as a protective shell that prevents the guest from dimerization or from the reaction with bulk phase reactants that are too large to pass through one of the portals in the host shell. The spectroscopic characterization of molecules with bent or twisted multiple bonds or with antiaromatic character is a very important field in theoretical and structural organic chemistry [21]. The taming of these highly reactive species has always been a special challenge for the experimentalist. For decades, highly sophisticated techniques have been developed for this purpose which mostly rely on matrix-isolations under cryogenic conditions or ultra-fast spectroscopy. The beauty of the container compound approach, however, is its simplicity.

#### 3.5.1. *Cyclobutadiene*

Cram and coworkers introduced this novel approach by stabilizing one of the most interesting and deeply studied reactive intermediates: cyclobutadiene **20**, the ‘Mona Lisa of organic chemistry’ (Figure 5) [22]. Cyclobutadiene is the prototypical example to verify the theory of aromaticity [23]. It has transient existence under normal working conditions and is stable only in cryogenic matrices at 8K where Orville L. Chapman recorded its FT-IR spectrum [24].

Cram and coworkers generated **20** photochemically from  $\alpha$ -pyrone **21** inside hemicarcerand **6**. If empty **6** and  $\alpha$ -pyrone are heated in refluxing chlorobenzene,  $\alpha$ -pyrone enters the inner phase of **6** to form the stable hemicarceplex **6·21**. Photolysis of this hemicarceplex with the unfiltered light of a Xenon arc lamp generated incarcerated cyclobutadiene and CO<sub>2</sub>. The latter was subsequently expelled out of the inner phase of **6**. If oxygen was excluded from the reaction mixture, cyclobutadiene was stable up to 60 °C!

This allowed for its first NMR spectroscopic investigation in solution. A sharp singlet for **20** at  $\delta$  2.27 ppm was observed, which is 3.03 ppm upfield from the ring proton of **22** [25], due to the shielding effect by the aryl units of the surrounding host.

The sharpness of the inward pointing methylene protons proved the singlet ground state of **20**. When oxygen was passed through a solution of **6·20**, **20** was oxidized in the inner phase to malealdehyde **23**, whose existence was confirmed by its characteristic carbonyl stretch at 1696 cm<sup>-1</sup> and its NMR spectra. If a solution of **6·20** was heated in a sealed tube at high temperatures for a short period, the guest escaped the protective shelter and dimerized to give cyclooctatetraene which

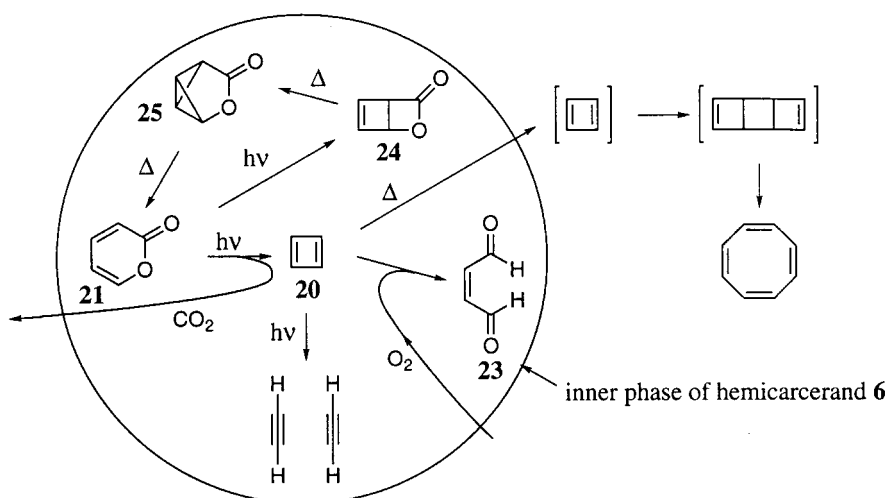
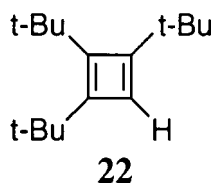


Figure 5. Photochemical and thermal inner phase reaction leading to cyclobutadiene stabilized by incarceration [22].



Scheme 2.

was revealed by its characteristic odor once the tube was opened. Prolonged photolysis of **6·20** split **20** into two acetylene molecules which escaped the inner phase and could be precipitated as red cuprous acetylide. Cram and coworkers further studied the mechanism of its formation by selective generation of the relevant intermediates. Photolysis with filtered light ( $\lambda > 300$  nm) converted **6·20** into photopyrone **6·24**, which as a solid, thermally rearranged at 90 °C into **6·25**. At higher temperature, **6·25** reverts quantitatively back to **6·21**.

These three photochemical and two thermal transformations were essentially quantitative. They took place in the same reaction environment: the inner phase. Cram proposed that these inner phases would allow in the future for the stabilization and examination of many other highly reactive species containing bent acetylenes and allenes, antiaromatic rings, radicals, or carbenes. He predicted correctly.

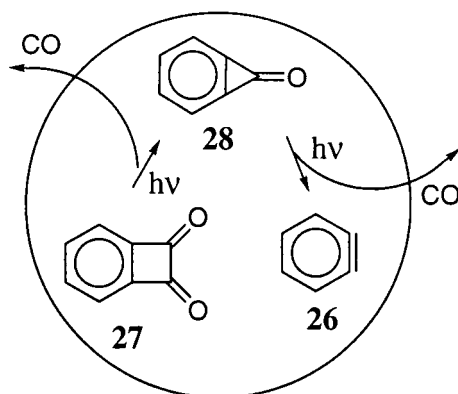


Figure 6. The two photochemical reactions leading to *o*-benzyne inside the inner phase of hemicarcerand **7** (symbolized with a circle) [28].

### 3.5.2. Benzocyclopropenone and *o*-benzyne

Almost half a century after Georg Wittig postulated didehydrobenzene **26** [26], and John D. Roberts proved undoubtedly its existence via  $^{14}\text{C}$ -labeling studies [27], this reactive intermediate could be stabilized by incarceration (Figure 6) [28].

The benzocyclobutenedione hemicarceplex **7·27** served as a precursor for the generation of incarcerated *o*-benzyne. Photolysis above 400 nm yielded the highly strained benzocyclopropenone **28**. The latter could be studied in solution only below  $-78\text{ }^\circ\text{C}$  [29]. However, protected from hydrolysis by the surrounding host shell, it was stable at room temperature, thus allowing for its X-ray crystal structure analysis [30]. The strong upfield shift of the H(2) of **28** ( $\Delta\delta = 3.48\text{ ppm}$ ) suggests that in the preferred guest orientation, its  $\text{C}_2$  axis is aligned with the long polar  $\text{D}_4$  axis of the host. In this orientation, the carbonyl group is deeply buried in the upper cavitation of **7**. This orientation would explain why incarcerated **28** hydrolyzes so slowly to form the benzoic acid hemicarceplex, despite its high reactivity and that water is small enough to reach into the inner phase. Here, we have another example of an inner phase protection from bulk phase reactants.

The photolysis of benzocyclopropenone has been studied in cryogenic matrices. Photolysis with unfiltered UV light extrudes CO to give *o*-benzyne, which photochemically equilibrates with cyclopentadienyldeneketene in the presence of CO [31]. Cyclopentadienyldeneketene is the dominant product at  $\lambda > 308\text{ nm}$ , but reverts back to *o*-benzyne and CO upon irradiation with light below 290 nm. Hence, the photolysis of **7·28** with filtered UV light at  $280 \pm 10\text{ nm}$  extruded CO and generated **26** of which a solution  $^1\text{H-NMR}$  spectrum could be recorded at  $-75\text{ }^\circ\text{C}$  (Figure 7) [28]. The assignment of the two guest proton signals at  $\delta 4.99\text{ ppm}$  and  $\delta 4.31\text{ ppm}$  was successful with a deuterium labeled 3-d-*o*-benzyne. As already mentioned for cyclobutadiene, the  $^1\text{H}$ -chemical shifts are strongly upfield shifted by the surrounding host. Under the assumption that the *o*-benzyne protons

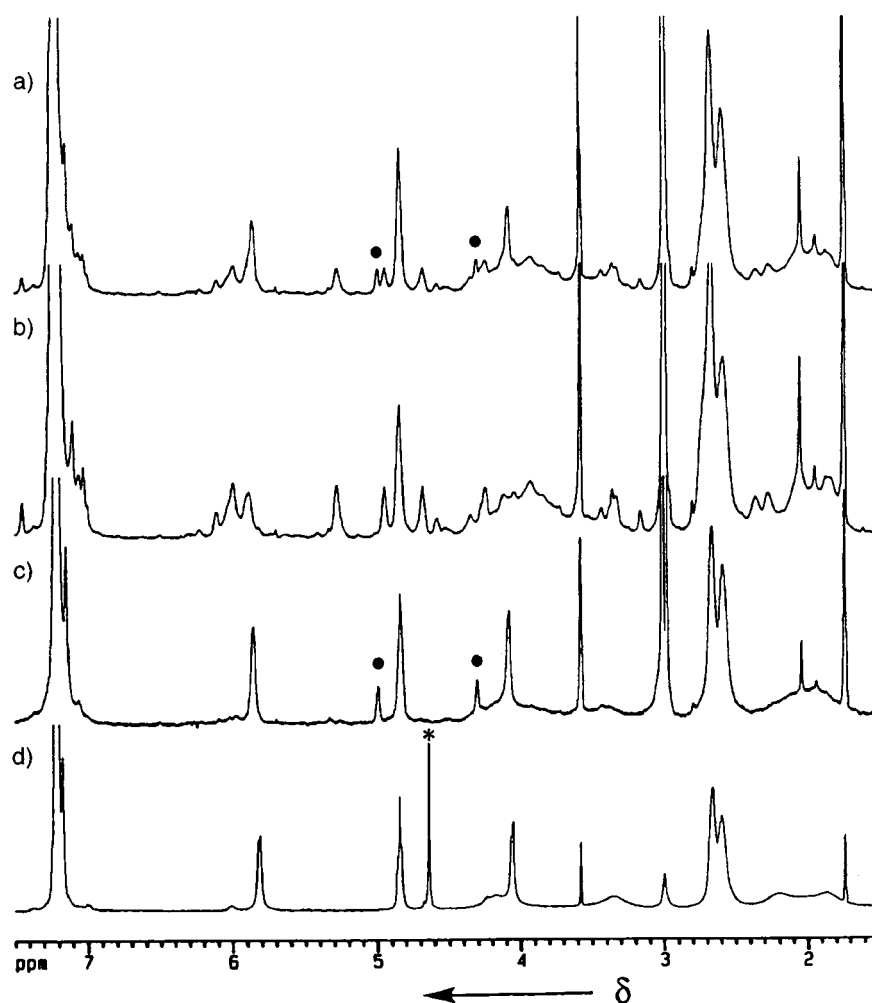


Figure 7.  $^1\text{H}$ -NMR spectra ( $[\text{D}_8]\text{THF}$ ,  $-75\text{ }^\circ\text{C}$ ) of (a) a photolyzed solution of **7·28** immediately after warming from  $-196\text{ }^\circ\text{C}$  to  $-75\text{ }^\circ\text{C}$ ; (b) after 30 minutes at  $-75\text{ }^\circ\text{C}$ ; (c) the *o*-benzyne hemicarceplex **7·26**; (d) the benzene hemicarceplex **7-benzene**. The peaks marked with black dots and an asterisk indicate the  $^1\text{H}$  nuclei of incarcerated *o*-benzyne and benzene, respectively. Reprinted with permission from *Angew. Chem.* 1997, **109**, 1406–1409; *Angew. Chem., Int. Ed. Engl.* 1997, **37**, 1347–1350. Copyright VCH Verlagsgesellschaft mbH, D-69451 Weinheim, 1997.

feel the same shielding by the surrounding host **7** as the protons of the structurally similar benzene [5h], the chemical shifts of “free” *o*-benzyne were estimated at  $\delta$  7.0 ppm and  $\delta$  7.6 ppm. Jiao *et al.* calculated the chemical shifts at the SOS-DFPT-PW91/III level [32]. The small deviation of  $\Delta\delta = 0.1$  ppm and 0.3 ppm, respectively between experiment and theory documents the high quality of this computational method.



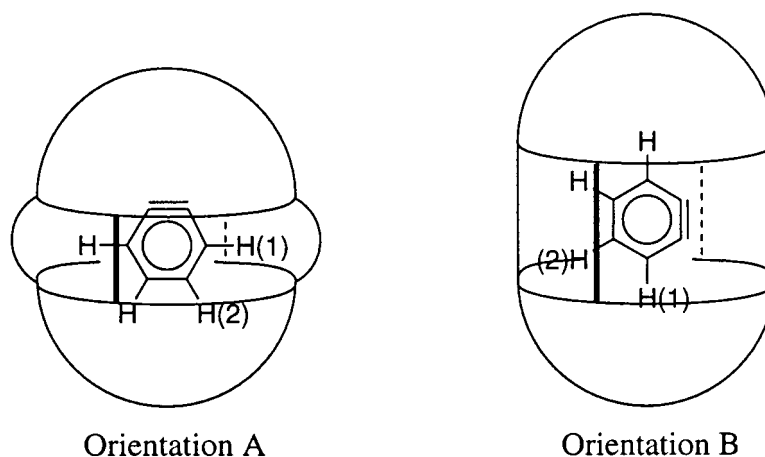


Figure 8. Two possible orientations of *o*-benzyne inside the inner phase of hemicarcerand **7**.

The chemical shifts of the guest protons showed a very strong temperature dependency [33]. This temperature dependency can be explained as the result of a change in the population of the two conformations **A** and **B** of the *o*-benzyne hemicarceplex (Figure 8). At low temperature, the two cavitands of **7** will come closer together in order to increase the number of van der Waals contacts between host and guest. This will change the shape of the inner phase such that it is complementary to *o*-benzyne in orientation **A** rather than to *o*-benzyne in orientation **B**. As a result of a higher thermal energy upon increasing the temperature, orientation **B** will be more populated. Hence, the *o*-benzyne protons H(1) will feel a stronger shielding by the host. On the other hand, the protons H(2), which are in the less shielded equatorial region of the host in orientation **B**, will experience a downfield shift. Orientation **A** explains why *o*-benzyne reacts very fast with an aryl ring of the host above  $-75\text{ }^{\circ}\text{C}$ , but does not react with water of the bulk solvent phase.

Much less relatively upfield shifted are the guest  $^{13}\text{C}$ -signals. Hence, they should provide more insight into the electronic properties of *o*-benzyne and also allow better comparison between calculation and experiment. A fully  $^{13}\text{C}$ -labeled *o*-benzyne was generated inside **7** and its  $^{13}\text{C}$ -NMR spectrum recorded at  $-98\text{ }^{\circ}\text{C}$  in  $\text{THF}_{d8}$  [28]. The measured chemical shift for the quarternary carbon of **26** at  $\delta$  181.33 ppm is within the experimental error of the average of the three chemical shift tensor principle values  $\delta$   $193 \pm 15$  ppm of matrix isolated  $^{13}\text{C}$ -enriched **26** at 20 K in argon [34]. The  $^{13}\text{C}$ -NMR spectrum of incarcerated *o*-benzyne also offered information about the  $^{13}\text{C}$ - $^{13}\text{C}$ -coupling. Comparison of the experimental  $^{13}\text{C}$ - $^{13}\text{C}$ -coupling constants with the coupling constants of model compounds suggested a cumulenic character of *o*-benzyne which, however, contradicts the most recent results of ab initio calculations [32]. They show no evidence for a pronounced bond length alternation necessary for a cumulenic structure of *o*-benzyne. From their calculation of the magnetic properties of *o*-benzyne, Jiao *et al.* concluded that *o*-

benzyne is aromatic according to its geometric, energetic and magnetic properties, and that the in-plane  $\pi$ -bond induces a small amount of bond localization resulting in an acetylenic character [32]. Nevertheless, the successful x-ray crystal structure analysis of the highly reactive benzocyclopropanone hemicarceplex leaves hope that in the nearest future a X-ray structure analysis of an *o*-benzyne hemicarceplex will unravel the 'real' structure.

### 3.6. INNERMOLECULAR DIELS–ALDER REACTION OF *o*-BENZYNE

In the cyclobutadiene hemicarceplex, no reaction between the guest and the host took place. However, the high reactivity of *o*-benzyne led to a Diels–Alder reaction with the surrounding host **7** [33].

This Diels–Alder reaction is slow enough below  $-75\text{ }^{\circ}\text{C}$  (half life time of 205 sec [28]) to allow for the recording of the  $^1\text{H-NMR}$  spectrum of *o*-benzyne but it reduces the guest's lifetime at room temperature to approximately 7 msec. In this bimolecular reaction, one reactant is completely encapsulated within the second reactant which also serves as a reaction vessel. It is referred to as an intramolecular reaction. In the intramolecular reaction, *o*-benzyne adds across the 1,4-position of one aryl unit of **7**. Although an intramolecular reaction is undesired if one's goal is the stabilization and characterization of a reactive intermediate, there are interesting aspects associated with it. An intramolecular reaction takes place at the concave inner surface of one reactant and is expected to be strongly affected by steric effects. Furthermore, the surrounding hemicarceplex constrains the guest mobility. This will have consequences for the entropy contributions to the activation barrier of an intramolecular reaction compared to a reaction in the liquid or gas phase. In addition, intramolecular reactions are expected to be independent of the bulk phase properties, as has already been observed for the photophysical properties of incarcerated biacetyl [17]. Intramolecular reactions can be used to probe topochemical effects that are seen, for example, in solids or rigid matrices (matrix effect) [35]. The reaction of incarcerated *o*-benzyne is very selective and only one product is formed [33]. In this case, the selectivity is a result of the large difference in the stability of the two possible regioisomers **29** and **30** [36].

However, the MM3\* minimum energy conformer of the *o*-benzyne hemicarceplex also shows a strong preorganization of the reactive triple bond for the observed Diels–Alder reaction with distances of 4.53 Å and 4.05 Å between the reacting *o*-benzyne carbons and the corresponding aryl carbons of **7**. A similar orientation was already deduced from the temperature dependency of the observed *o*-benzyne proton chemical shifts [33]. The high preorganization is a result of the rigidity of the inner phase and is reflected in the measured activation entropy  $\Delta S_{\text{expt}}^{\ddagger}(298\text{ K})$  of  $-10.7\text{ cal mol}^{-1}\text{ K}^{-1}$  [33]. The  $\Delta S_{\text{expt}}^{\ddagger}$  compares well with the activation entropy of the Cope rearrangement of hexatriene ( $\Delta S_{\text{expt}}^{\ddagger}(298\text{ K}) = -6.05\text{ cal mol}^{-1}\text{ K}^{-1}$ ) [37] or the intramolecular Diels–Alder reaction of triene **31** ( $\Delta S_{\text{expt}}^{\ddagger}(298\text{ K}) = -14.4\text{ cal mol}^{-1}\text{ K}^{-1}$ ) [38]. Beno *et al.* calculated the activation

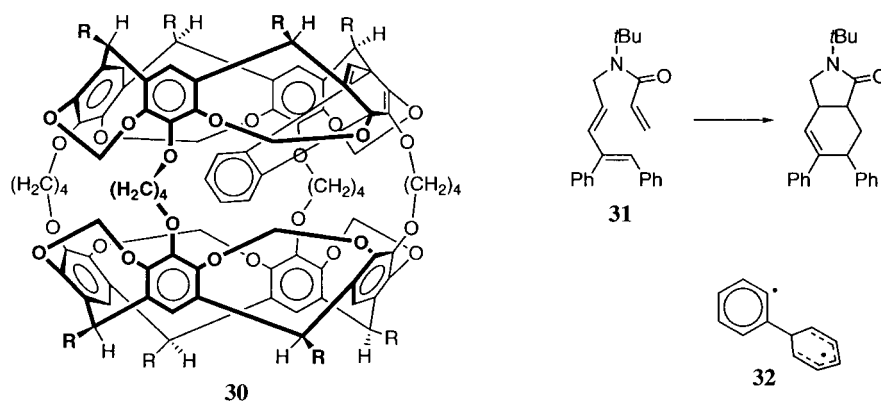


Chart 7.

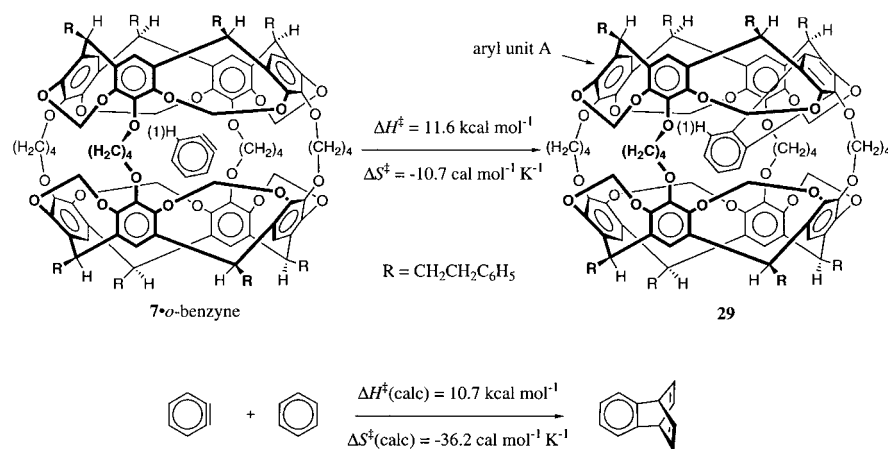


Figure 9. Comparison of the kinetic activation parameters of the intramolecular Diels-Alder reaction between *o*-benzyne and the surrounding hemicarcerand **7** [33] with the calculated energies for the Diels-Alder reaction between *o*-benzyne and benzene [36].

parameters for the Diels-Alder reaction between *o*-benzyne and benzene on the Becke3LYP/6-31G\* level (Figure 9) [36]. Interestingly, the  $\Delta H_{\text{calc}}^{\ddagger}$  of 10.7 kcal mol<sup>-1</sup> compares very well with the experimental  $\Delta H_{\text{expt}}^{\ddagger}$  of 11.6 kcal mol<sup>-1</sup> of the intramolecular reaction. The fact that the electron donating substituents of the aryl unit of **7** will certainly increase its reactivity relative to benzene, shows that the increased reactivity of **7** must be compensated by steric repulsion in the transition state leading to **29**. The MM3\* optimized structure of **29** reveals the origin of such steric repulsion [36]. Although the phenyl unit is not located in a too crowded environment compared to the regioisomer **30**, the phenyl-H(1) in **29** experiences some repulsive interaction with the aryl unit A which should be felt in the transition state, too. The proximity to the aryl unit A causes the large upfield shifted chemical shift of H(1) ( $\delta$  3.12 ppm). In addition, Beno *et al.* calculated the activation

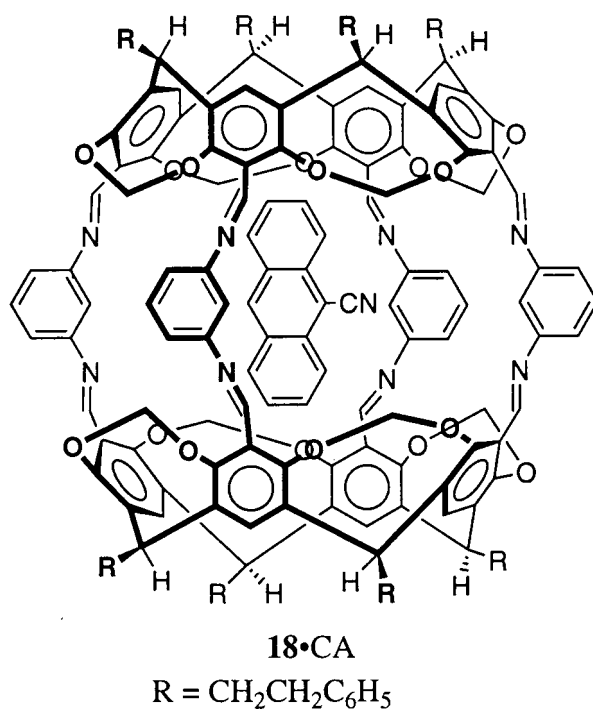


Chart 8.

barriers for a stepwise Diels-Alder reaction between *o*-benzyne and benzene [36]. The  $\Delta H_{\text{stepwise}}^{\ddagger}$  is only 2.4 kcal mol<sup>-1</sup> higher than for the concerted pathway. The above mentioned repulsive interactions in the innermolecular reaction transition state should be larger for a concerted pathway than for a stepwise pathway with the intermediary formation of biradical **32**. This highly suggests, that the steric constraint imposed by the surrounding host changes the reaction mechanism in the inner phase from a concerted pathway to a stepwise biradical pathway. This hypothesis awaits further experimental and computational efforts.

### 3.7. STABILIZATION OF EXCITED STATES BY INCARCERATION

The photophysical properties, in particular the excited state life-time of molecules enclosed in constrained media such as cyclodextrins or zeolites, have always been of great interest due to the possibility to develop novel photophysical probes for immuno assays, information storage devices, or solar-energy conversion devices [39]. Hemicarcerands are a very interesting new class of constrained media. Their molecular skeleton can interact with the incarcerated guest and also forms an “insulating” skin preventing a direct contact between the guest and bulk phase components. Parola *et al.* investigated the photophysical properties of 1-cyano-anthracene (CA) incarcerated in hemicarcerand **18** [40].

They observed remarkable differences in the photophysical properties of incarcerated CA compared to free CA. The surrounding host caused a red-shift of the absorption spectrum of CA and also reduced the lifetime of the singlet excited state  $^1L_a$  by a factor of 40. In addition, the quantum yield was 50 times smaller for incarcerated CA compared to free CA. An energy transfer between the host and the guest, however, was observed only with negligibly small efficiency (<3%) upon selective excitation of **18**. Furthermore, the insulating surrounding host-shell completely prevented a fluorescence quench by the bulk phase quencher 1,5-diazabicyclo[4.3.0]non-5-ene (DBN). Since no overlap between the guest emission bands and the host absorption bands was observed, energy transfer quenching from the host to the guest can be ruled out. Parola *et al.* concluded that the electron transfer quenching would be most likely caused by the methoxybenzene units of **18** and estimated that such electron transfer would be exothermic. Based on this result, they suggested that this hemicarceplex might lead to a new class of highly efficient luminescence labels for immuno assays. Further studies from this group [17] and independently by Farrán and Deshayes [16] with triplet sensitizer biacetyl incarcerated in host **19** provided more insight into the role of the host on the lifetime of excited states. The measured lifetime of the  $T_1$  excited state of incarcerated biacetyl in solution was almost twice as large as the lifetime of free biacetyl in solution and unaffected by the nature of the solvent. Even more interesting, despite its small size, dioxygen was virtually unable to quench the phosphorescence of incarcerated biacetyl. The dioxygen quenching rate was estimated to be  $10^6$  times smaller than for free biacetyl. The  $T_1$  excited state life-time of incarcerated biacetyl, which is longer than the life time of free biacetyl in the liquid phase, but shorter than the lifetime in the gas phase, was interpreted as incarcerated biacetyl being in a not-too-tight cavity. This provides more free space with less specific cage-guest interactions, compared to a solvent cage. But it still causes a higher number of collisions of the incarcerated  $T_1$  excited state with the surrounding host walls compared to the gas phase.

### 3.8. THERMAL REACTIONS

A very interesting thermal retro-Diels-Alder reaction inside the asymmetric carcerand **33** [7h-j] was recently reported by Reinhoudt and coworkers. They studied the extrusion of  $SO_2$  and butadiene from an incarcerated 3-sulfolene carceplex **33**·3-sulfolene by electron impact mass spectroscopy (EI-MS) and field desorption mass spectrometry (FD-MS) [7j].

The extrusion of  $SO_2$  and butadiene from free 3-sulfolene readily takes place at 100–130 °C. However, when the probe was loaded with the carceplex **33**·3-sulfolene and gradually heated up,  $SO_2$  was detected by EI-MS only above 170–180 °C, and butadiene at 215 °C. The FD-MS showed only the intact carceplex up to temperatures of 180 °C. Above 180 °C, the empty carcerand was also detected, but neither a  $SO_2$  carceplex, nor a butadiene carceplex was observed.

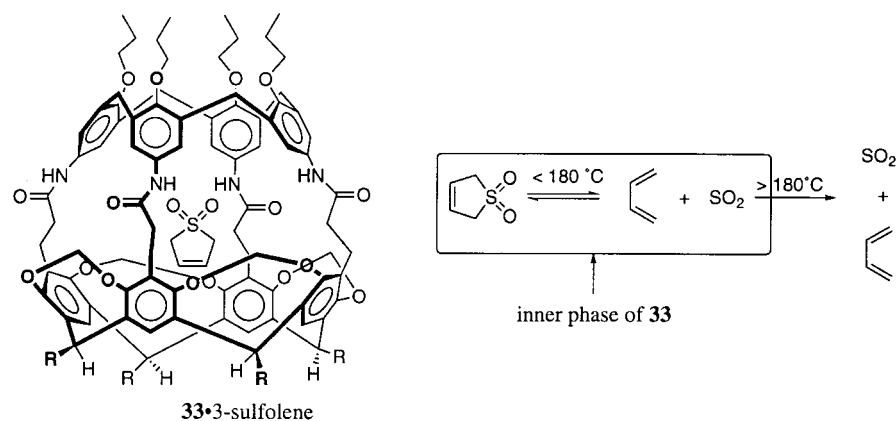


Chart 9.

Since this host is stable at such high temperatures, guest escape due to the thermal destruction of **33** can be excluded. Hence, the detected  $\text{SO}_2$  and butadiene must result from **33•3-sulfolene** and must escape from the inner phase through one of the larger side portals. Reinhoudt explained the unusually high thermal stability of incarcerated 3-sulfolene with a fast recombination rate for the extrusion products in the inner phase. Below  $180^\circ\text{C}$ , a thermal equilibrium between 3-sulfolene,  $\text{SO}_2$  and butadiene is established, which is pulled towards the extrusion products via their escape from the inner phase above  $180^\circ\text{C}$ . This shows impressively how the confined inner phase changes the rates of bimolecular reactions by providing a very high local concentration of both reactants. Several more of such bimolecular inner phase reactions will be discussed in Section 5.

#### 4. Molecular Lantern and Reaction Bowls

The exact opposite of an intramolecular reaction is the cleavage of an endohedrally anchored functional group leading to an encapsulated guest molecule. This new principle of supramolecular complex formation was developed and first realized by Renji Okazaki and his coworkers [41]. Using this principle, highly reactive intermediates incarcerated or endohedrally fixed inside a container compound can be generated and are protected from self-destruction. Okazaki *et al.* noticed the ability of enzymatic binding sites to stabilize highly unstable and reactive species by preventing their self-destruction or oligomerization via the protein framework around the active site. For example, sulfenic acids  $\text{R-S-OH}$  are unstable in the bulk due to rapid self-destruction reactions leading to thiosulfonates  $\text{R-S(O)-SH}$ , disulfides  $\text{R-S-S-R}$  or sulfonic acids  $\text{R-SO}_2\text{H}$  [42, 43]. However, it has been suggested that the oxidation of cysteinyl side chains in the active site of papain or glyceraldehyde-3-phosphate dehydrogenase leads to stable cysteine sulfenic acid  $\text{Cys-SOH}$  which is unable to react with another  $\text{Cys-SOH}$  or  $\text{Cys-SH}$  moiety [43a]. With the aim

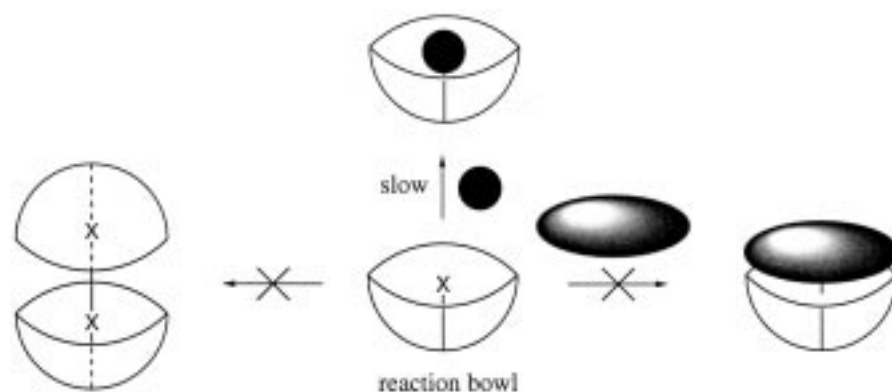


Figure 10. Schematic representation of an endohedral functional group X inside a *reaction bowl*. The reaction bowl prevents the dimerization of X and its reaction with large bulk phase reactants, but allows for a selective reaction with small bulk phase reactants.

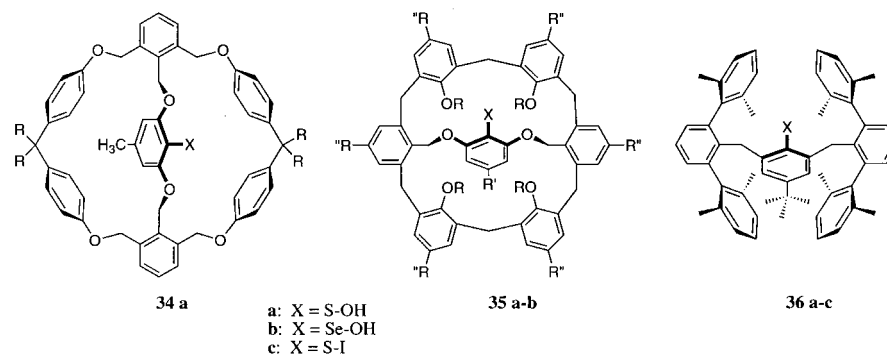


Chart 10.

to simulate the sulfenic acid stabilization in enzyme binding sites, Okazaki *et al.* developed a new type of compound which they referred to as *reaction bowls*.

Reaction bowls have a functional group embedded in a deep concave bowl-shaped cavity [44]. If this functional group is highly reactive, the surrounding bowl prevents its dimerization or oligomerization, but leaves it still exposed to the bulk medium. This design is particularly elegant for the mimicking of enzyme active sites. Three types of reaction bowls have been successfully prepared. These bowls are based on bridged cyclophanes **34** [45], bridged calix[6]arenes **35** [46], or the acyclic 4-*tert*-butyl-2,6-bis[(2,2'',6,6''-tetramethyl-*m*-phenyl-2'-yl)methyl]phenyl group **36** [47], each with an aryl group X, shielded by the surrounding carbon skeleton.

To prove the initial hypothesis, Okazaki *et al.* transformed the X-group of each reaction bowl chemically into a sulfenic acid group. The sulfenic acid group in **34a** [45], **35a** [46a], and **36a** [48] were stable far above ambient temperature, protected from dimerization and self-destruction by the steric demand of the sur-

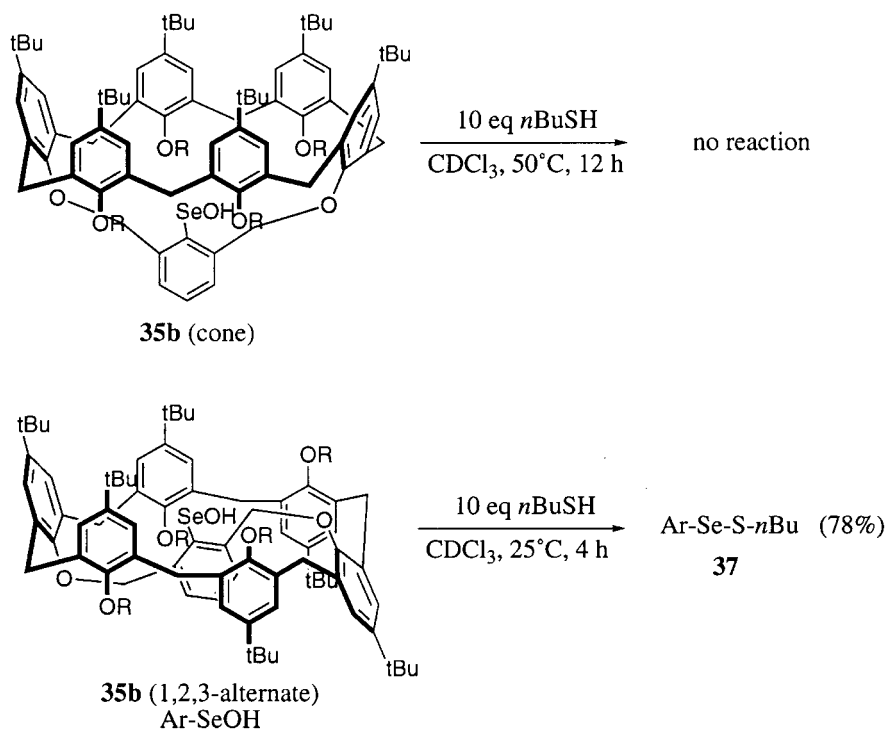


Chart 11.

rounding bowl. The presence of stable sulfenic acid groups was confirmed via X-ray structure determinations of **35a** [46a] and **36a** [48]. Despite its inability to react with another sulfide or sulfenic acid group embedded in another reaction bowl, the sulfenic acid group was still accessible for small bulk phase reactants. Oxidation of the sulfenic acid group to a sulfinic acid function was possible with *m*-chloroperbenzoic acid, as well as the reaction with 1-butanethiol to afford disulfides, but with a strongly reduced rate compared to the parent reaction of free sulfenic acids [45, 48]. Using the same reaction bowls, Okazaki *et al.* prepared stable selenic acids **35b** [46d] and **36b** [41] and most recently a stable sulfonyl iodide derivative **36c** [49], which was protected from disproportionation. The geometric features of these very delicate functionalities were successfully investigated *via* X-ray crystallographic structure determinations [46d, 49]. A conformation dependent reactivity towards external sulfides was observed for the selenic acid inside calix[6]arene reaction bowl **35b** [41]. In the 1,2,3-alternate conformation, 1-butanethiol led at room temperature to selenylsulfide **37** whereas no reaction was observed in the cone conformation even at higher temperatures. This suggests that the tailoring of the reaction bowl rims and of the orientation of the embedded functional group within the cavity can result in high structural recognition and selection for bulk phase reactants.



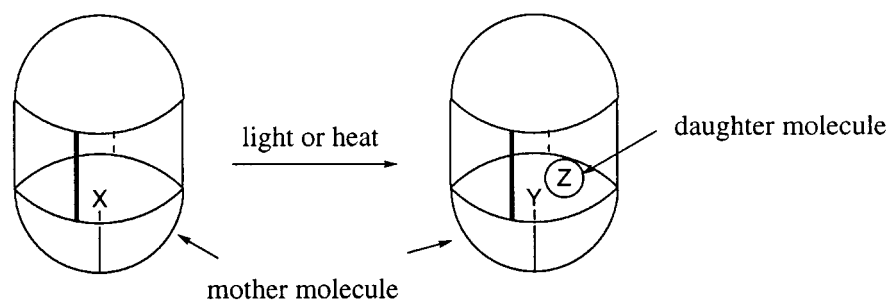


Figure 11. Schematic representation of the *mother molecule–daughter molecule complex* formation via photolysis or thermolysis of a *lantern molecule*.

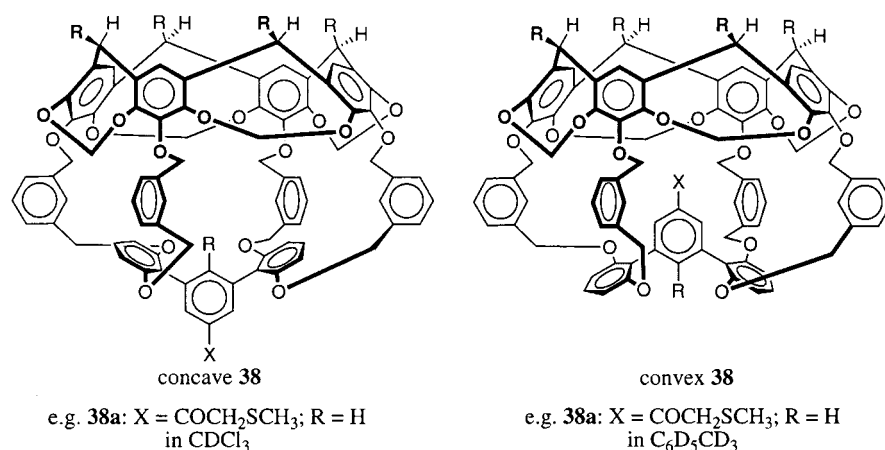


Chart 12.

An extension of the concept of reaction bowls are *molecular lanterns* **38** [50, 51]. They are derived by capping a reaction bowl with a cavitand. This design leads to a completely encapsulated endohedral functionality, which cannot self-destruct and is even more shielded from the bulk medium than in a reaction bowl.

Molecular lanterns **38** adopt two distinct conformations. In their concave conformation, the X-group is exohedral, whereas the X-group is deeply buried in the inner cavity of the upper cavitand in the convex conformation. Which conformation is preferred depends largely on the steric demand of X. For X = COCH<sub>2</sub>SCH<sub>3</sub> and R = H **38a**, the chemical shift of the thiomethyl group suggests that the molecular lantern is in the concave conformation in CDCl<sub>3</sub> ( $\delta$  2.19 ppm), but in the convex conformation in [D<sub>8</sub>]toluene ( $\delta$  -1.22 ppm) [51].

Okazaki *et al.* applied the molecular lantern **38a** for the stabilization of reactive intermediates [51]. The photochemical cleavage of the endohedral methylthioacetate group lead to thioformaldehyde **39** encapsulated in the inner phase of the surrounding lantern **40**. Since in this complex, the guest has not been introduced from the outer bulk medium, but via bond cleavage from the inner surface of the

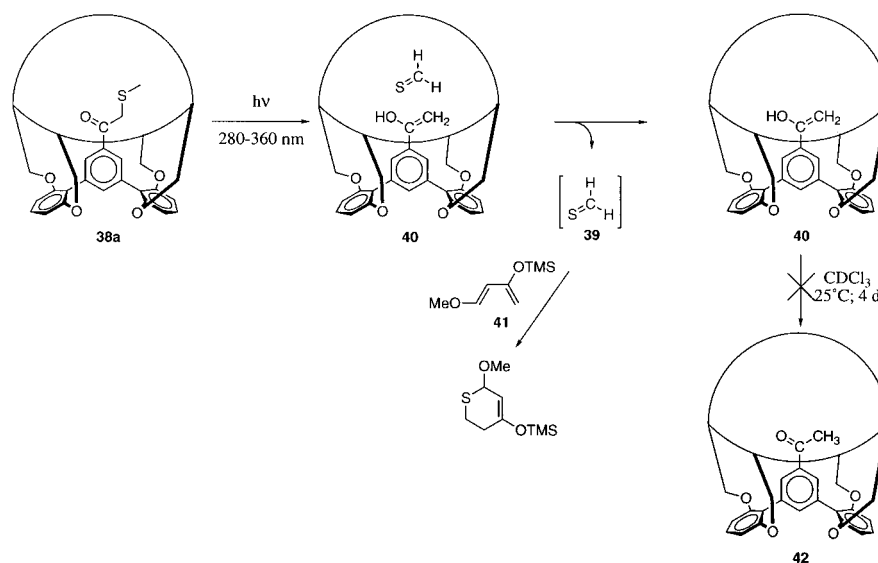


Chart 13.

lantern, Okazaki *et al.* suggested the name ‘*mother molecule–daughter molecule*’ complex for these compounds.

The thioformaldehyde guest could be chemically trapped in the bulk phase with Danishefsky’s diene **41** after it escaped the inner phase. Despite its extreme instability, the encapsulated thioformaldehyde had a much longer life-time, protected by the surrounding cage, and could still be captured 7 seconds after the photolysis was complete. More interestingly, the photochemical reaction left behind an endohedral monosubstituted enol **40**, which for the first time allowed for its chromatographic purification and isolation without any observed tautomerization. This endohedrally protected enol resisted ketonization to **42** at room temperature in  $\text{CDCl}_3$  for more than four days. It required three days to reach completion in the presence of trifluoroacetic acid, which would instantaneously tautomerize any simple free enol. Goto and Okazaki proposed that the principle of mother molecule–daughter molecule complexes would lead in the future to the stabilization of many reactive intermediates, fixed within the capsule and almost completely isolated from the bulk [41]. Also, novel delivery systems based on the structural framework of lantern molecules can be envisioned in which an intense brief stimulus generates a daughter molecule which is then slowly released into the bulk on a controlled rate which depends on the shape and size of the openings in the mother molecule.

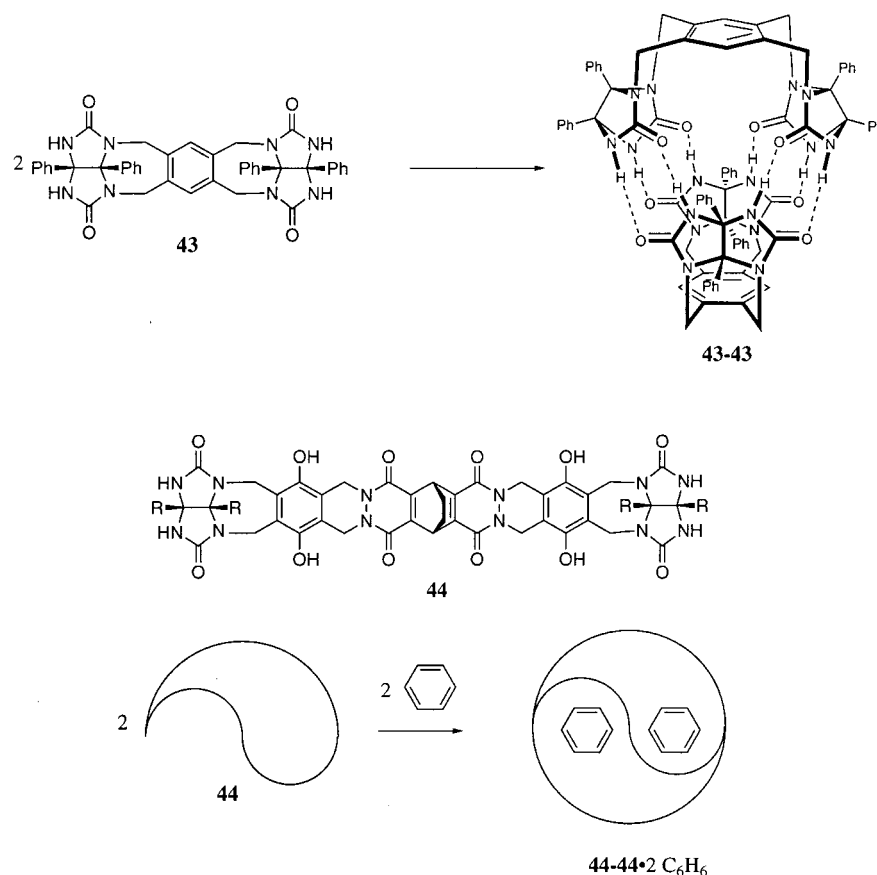


Chart 14.

## 5. Self-Assembled Capsules as Reaction Catalysts

The high local concentration of both reactants is the underlying principle of the rate enhancing effect of H-bond stabilized self-assembled capsules on several Diels-Alder cycloadditions [52]. In 1993, Wyler, de Mendoza and Rebek introduced self-assembled molecular containers [53a]. The two concave shaped halves **43** are held together via multiple weak hydrogen-bond interactions and form a “softball” like closed-shell capsule **43-43** around an inner space that can accommodate one or even more small organic guest molecules. As a result of the non-covalent bonds that hold these capsules together, guest binding and exchange is a dynamic process, which can be detected and followed by solution phase NMR. In analogy to the formation of Cram’s hemicarcerands via shell-closure reactions, the formation of a dimeric capsule requires templation by a guest molecule and shows also high structural recognition [54]. Over the past years many different dimeric capsules have been synthesized and studied [53].

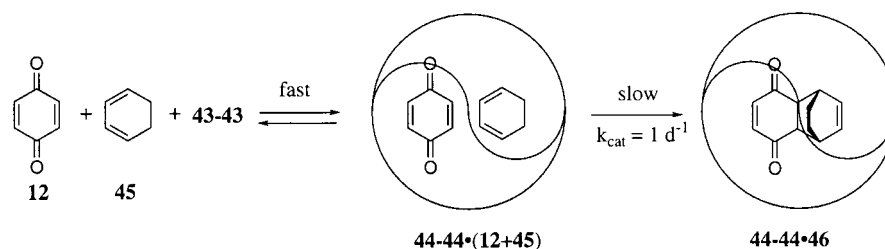


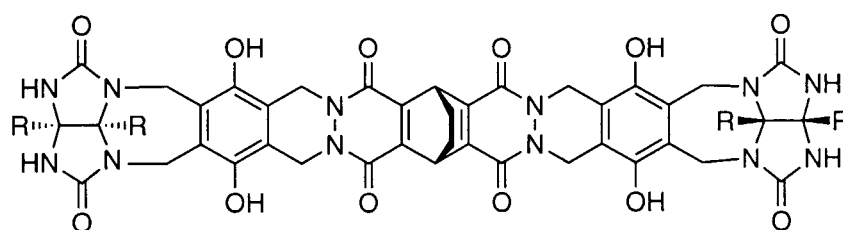
Chart 15.

Particularly, the dynamics of guest binding and the simultaneous binding of two molecules of benzene inside capsule **44-44** [53n], lured Kang and Rebek to investigate the possibility to use capsules as novel reaction vessels for bimolecular reactions [55]. They studied the effect of **44** on the Diels-Alder reaction between *p*-quinone **12** and cyclohexadiene **45** [55b, c]. In the absence of **44**, using millimolar concentrations of both reactants, the half-life of the reaction between free **12** and **45** could not be measured but was anticipated to be one year. However, if the dimeric capsule **44-44** (1 mM) is added to a solution of both reactants (4 mM), the product complex **44-44-46** slowly formed within one day as followed by the change in the  $^1\text{H-NMR}$ .

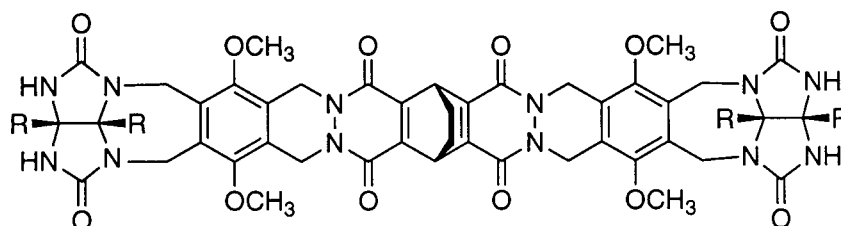
From an analysis of the initial rate, approximately a 200-fold rate acceleration was determined. Kang and Rebek compared the proposed initial tetrameric complex **44-44-12 + 45** as an analog of a Michaelis complex in enzyme catalyzed reactions. Consistently, upon varying the cyclohexadiene concentration, saturation kinetics was observed. A Lineweaver-Burk plot revealed a  $V_{\text{max}}$  of  $0.001 \text{ M}^{-1} \text{ d}^{-1}$  and a  $k_{\text{cat}}$  of  $1 \text{ d}^{-1}$ . Clearly the strong binding of **46** by the capsule prevented turnover. Similarly, other potential guests, such as benzene or [22]-paracyclophane, when added to the reaction mixture, completely inhibit the accelerating effect of the capsule. The belief that the rate acceleration is truly a result of the encapsulation and not due to a catalysis by the phenolic hydrogens of **44** was proven with the kinetic results obtained in the presence of **47** and **48**.

No rate acceleration was observed for **47**, which has the same functional groups as **44**. However, its S-shape does not allow dimeric capsule formation. Also **48**, which has the same shape as **44** but whose methoxy groups sterically prevent capsule formation, showed no rate acceleration. In addition, **44-44** does neither accelerate the corresponding reaction of the larger naphthoquinone **49**, which cannot be encapsulated together with **45**, nor the reaction between **12** and cyclopentadiene **50**, which is too small to form a favorable complex.

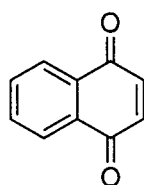
All of this suggests the necessity of encapsulation. To find the origin of the rate acceleration, Kang and Rebek estimated that the local concentration of each reactant inside the capsule would be five molar, over 1000-fold higher than the concentration of the reactants in the bulk. Hence, the enhanced concentration of the reactants is most likely the reason for the increased rate of the Diels-Alder



47



48



49



50

Chart 16.

reaction rather than a particular stabilization of the transition state compared to the reactants as in antibody catalyzed Diels-Alder reactions. Rebek *et al.* proposed that true catalysis via encapsulation could be possible if the clever design would allow a stronger stabilization of the transition state, compared to the reactants [55b].

In order to find a real turn-over catalyst, Rebek and coworkers further investigated other Diels-Alder reactions with the hope of finding a system in which the Diels-Alder adduct would be less strongly bound than the reactants. For example, turn-over would result if the primary Diels-Alder adduct could be altered in a subsequent reaction step leading to a secondary product that is less strongly bound by the capsule. This approach was successfully applied before by Hilvert for an antibody catalyzed Diels-Alder reaction [56]. With this hypothesis in mind, Rebek and coworkers studied the reaction between **12** and thiophene dioxide **51**. They hoped that SO<sub>2</sub> extrusion from the primary Diels-Alder adduct **52** would reduce the capsule's affinity for the product and would result in turn-over [55a]. And indeed, turn-over was observed, however, as the result of a different driving force. In the presence of 10 mol% of the dimeric capsule **44–44**, pseudo-first-order

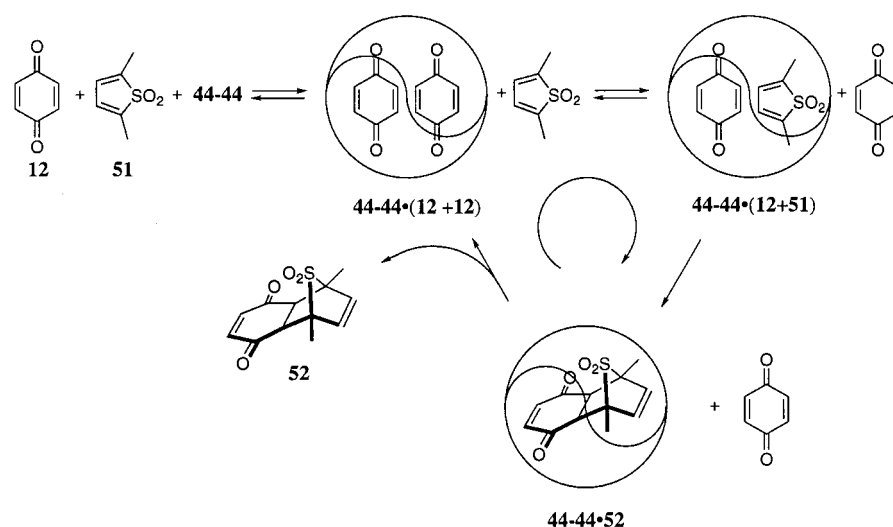


Figure 12. Catalytic cycle of the formation of **52** via an inner phase Diels-Alder reaction between *p*-quinone **12** and thiophene dioxide **51** encapsulated inside a "softball" **44-44** [55a].

kinetics were observed over two half-life times which indicated that no product inhibition took place, but true catalysis leading to a 10-fold rate enhancement. This corresponds to more than seven turn-overs by the capsule. The driving force for this turn-over is the stronger binding of two molecules of **12** by the capsule compared to the product **52**.

Although the overall acceleration was modest, the key point has been proven: catalysis. Rebek proposed that self-assembled molecular capsules might have a promising future as catalytic reaction chambers.

## 6. Fullerenes

Since their somewhat spectacular discovery, fullerenes have received much attention among the scientific community [57]. Fullerenes are a novel modification of carbon with spherical inner cavities surrounded by a carbon skeleton which, unlike that of carcerands, has no openings. The inner cavity dimensions of fullerenes, with diameters larger than 3.5 Å, make them suitable for the incarceration of small molecules and single atoms. Several endohedral fullerene complexes containing metal cations [58] or noble gas atoms [59] have been generated and characterized. Some of these show very interesting physical properties. For example, the alkali metal salts of C<sub>60</sub> exhibit superconductivity (K<sub>3</sub>C<sub>60</sub>, *T<sub>c</sub>* = 18 K, Rb<sub>3</sub>C<sub>60</sub>, *T<sub>c</sub>* = 30 K) [60], ferromagnetism (*T<sub>c</sub>* = 16 K) in the charge transfer salt with ((CH<sub>3</sub>)<sub>2</sub>N)<sub>2</sub>C=C(N(CH<sub>3</sub>)<sub>2</sub>)<sub>2</sub> [61], and third-order optical non-linearity [62]. Only one example of a non-metal and non-noble gas endohedral fullerene complex, which is the recently reported endohedral nitrogen complex of C<sub>60</sub>, N@C<sub>60</sub>, has been prepared [63]. However, this complex is particularly interesting. EPR and ENDOR stud-

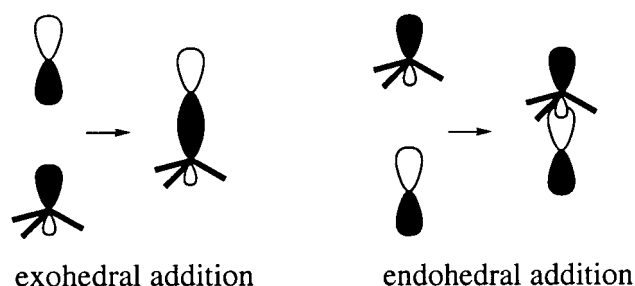


Figure 13. Schematic representation of an exohedral (left) or endohedral addition (right) of the  $p$ -orbital of nitrogen to a carbon of the  $C_{60}$  cage.

ies confirmed that this fullerene contains the nitrogen atom in its ground state ( $^4S_{3/2}$ ), and not covalently bound to the fullerene cage as one would immediately expect for such a reactive species [63]. This suggests that, unlike the outer surface, the inner surface of a fullerene exhibits an unusual inertness. Hirsch *et al.* performed semiempirical (PM3-UHF/RHF) and density functional calculations (UB3LYP/D95\*/PM3) in order to find an explanation for the passiveness of the inner fullerene surface [64]. They calculated the energy profile for the approach of the doublet state of the endohedral N atom to a carbon atom, a [5, 6] bond, or a [6, 6] bond of the cage. Local energy minima were located for each approach. However, the energies of the resulting adducts are 20–50 kcal/mol higher than doublet state  $N@C_{60}$ , which is calculated to be 22 kcal/mol above the quartet ground state.

This is in vast contrast to an attack of N to the exohedral surface, which is known to easily undergo addition reactions to form stable exohedral adducts [65]. On the molecular orbital level, this different reactivity can be explained as a result of the concavity. Here concavity leads to an average  $\sigma$ -bond hybridization of  $sp^{2.28}$  [66], a partial  $s$ -character of the  $\pi$ -orbitals, and a higher charge density on the outer surface of  $C_{60}$  due to fewer electron repulsions compared to the endohedral surface. Upon an endohedral addition, the nitrogen and carbon orbitals poorly overlap. Further destabilization results from valence electron repulsions and unfavorable geometries. The exohedral nitrogen addition, however, leads to the exact opposite effect – a less strained addition product (Figure 13).

Interestingly, the calculated energy barriers for the penetration of the doublet N from the interior through a [5, 6] or a [6, 6] bond are rather low (49 and 41 kcal/mol, respectively) compared to the most favorable calculated barrier for He escape out of  $He@C_{60}$  (225 kcal/mol) [67]. Helium escape requires temperatures higher than 600 °C and is accompanied by permanent cage destruction [59a–d]. However, based on these calculations, an autocatalytic non-destructive dissociation pathway as outlined in Figure 14 should exist for  $N@C_{60}$ . Hirsch *et al.* tested this hypothesis experimentally. Indeed, when  $N@C_{60}$  was heated to 260 °C, the EPR signal continuously decreased, suggesting that the N guest must have penetrated

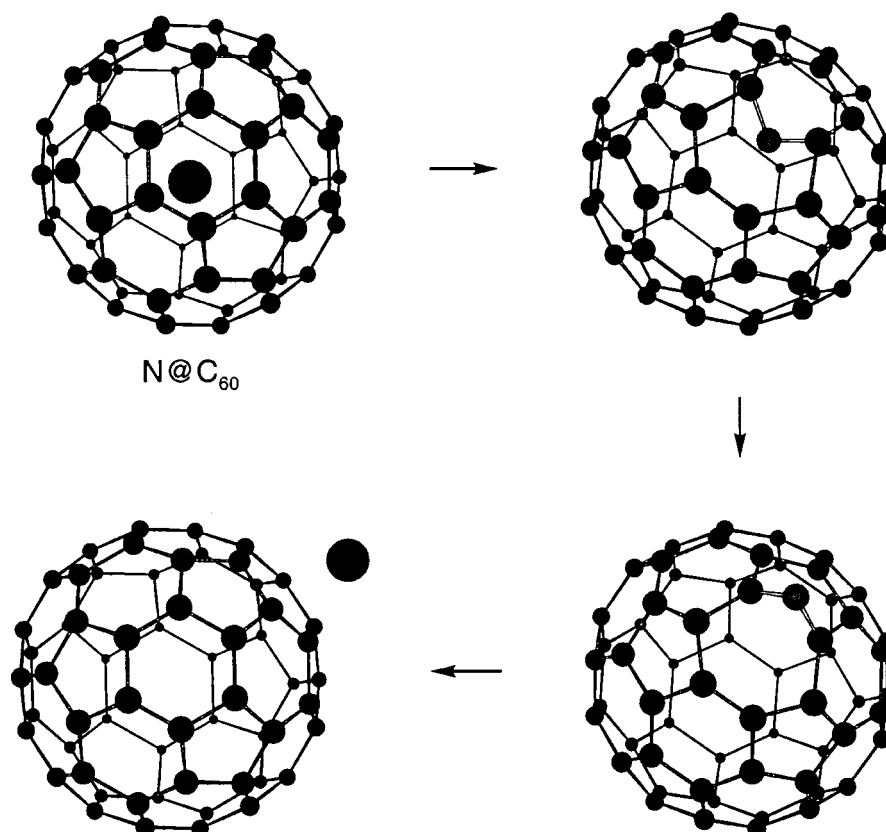


Figure 14. The autocatalytic escape of endohedral quartet nitrogen out of  $C_{60}$  via an endohedral and an exohedral nitrogen- $C_{60}$  adduct [64].

the cage leading to diamagnetic products. The activation energy was estimated at 40 kcal/mol from the decrease in intensity with time.

The unexpected low reactivity of the inner surface of fullerenes, which Hirsch *et al.* called a ‘chemical Faraday cage’, makes them particularly attractive for the investigation of other reactive atoms or even molecules. Taking into account the recent successes in the isolation of higher fullerenes, in synthesizing them via ‘wet chemical methods’ and in ‘cracking’ them open [68], we can expect in the future many other interesting studies of reactive species inside the inert inner phases of fullerenes.

## 7. Conclusions

The large variety of different reactions which have been summarized in this review, and the ability of photons, electrons, and protons to pass through the shell of a molecular container clearly shows that the inner phases are a new and highly in-



teresting environment for chemical reactions. Container compounds not only open up new avenues for the design of delivery systems, molecular switches or other photophysical devices, but they will certainly be used in the future as catalysts which show all the positive features of enzymatic catalytic binding pockets. Important steps toward this goal are the observation of the high structural selection in through-shell alkylations and hydrogen transfer reactions, and the demonstration of turn-over in molecular capsule-mediated Diels-Alder reactions. In the light of the fast development of new hemispherical and self-assembled capsules with different shapes, sizes and solubility properties, we can expect many more interesting examples of inner phase reactions in the future.

Furthermore, the photochemical or thermal generation of highly reactive intermediates in the inner phases of molecular containers and their stabilization by incarceration will always play an important role in the investigation of reaction mechanisms and in the structural and electronical characterization of highly unstable or strained organic molecules.

### Acknowledgements

The author would like to thank all of his coworkers for their efforts to advance this exciting research field and for proofreading this manuscript. He warmly thanks the National Institute of General Medical Sciences (grant R01 GM57934-01) and Kansas State University at Manhattan for generous financial support of his research.

### References

1. (a) D. J. Cram: *Science* **219**, 1177 (1983). (b) D. J. Cram: *Nature* **356**, 29 (1992); (c) D. J. Cram and J. M. Cram: *Container Molecules and Their Guests*, (Monographs in Supramolecular Chemistry, No. 4, Series Editor J. F. Stoddart) The Royal Society of Chemistry, Cambridge, U.K. (1994).
2. D. J. Cram: *Angew. Chem., Int. Ed. Engl.* **27**, 1009 (1988).
3. (a) D. J. Cram, S. Karbach, Y. H. Kim, L. Baczynskyj, and G. W. Kallemeyn: *J. Am. Chem. Soc.* **107**, 2575 (1985). (b) D. J. Cram, S. Karbach, Y. H. Kim, L. Baczynskyj, K. Marti, R. M. Sampson, and G. W. Kallemeyn: *J. Am. Chem. Soc.* **110**, 2554 (1988).
4. (a) J. C. Sherman and D. J. Cram: *J. Am. Chem. Soc.* **111**, 4527 (1989). (b) J. C. Sherman, C. B. Knobler, and D. J. Cram: *J. Am. Chem. Soc.* **113**, 2194 (1991).
5. (a) J. A. Bryant, M. T. Blanda, M. Vincenti, and D. J. Cram: *J. Am. Chem. Soc.* **113**, 2167 (1991). (b) L. C. Q. Quan and D. J. Cram: *J. Am. Chem. Soc.* **113**, 2754 (1991). (c) Q. C. L. Quan, C. B. Knobler, and D. J. Cram: *J. Chem. Soc., Chem. Commun.* 660 (1991). (d) D. J. Cram, M. E. Tanner, and C. B. Knobler: *J. Am. Chem. Soc.* **113**, 7717 (1991). (e) D. J. Cram, M. T. Blanda, K. Paek, and C. B. Knobler: *J. Am. Chem. Soc.* **114**, 7765 (1992). (f) H. J. Choi, D. Buhning, M. L. C. Quan, C. B. Knobler, and D. J. Cram: *J. Chem. Soc., Chem. Commun.* 1733 (1992). (g) D. J. Cram, R. Jaeger, and K. Deshayes: *J. Am. Chem. Soc.* **115**, 10111 (1993). (h) T. Robbins, C. B. Knobler, D. Bellew, and D. J. Cram: *J. Am. Chem. Soc.* **116** (1994), 111. (i) C. Eid Jr., C. B. Knobler, D. A. Gronbeck, and D. J. Cram: *J. Am. Chem. Soc.* **116**, 8506 (1994). (j) C. Von dem Buschehunnfeld, D. Buhning, C. B. Knobler, and D. J. Cram: *J. Chem.*

- Soc., Chem. Commun.* 1085 (1995). (k) Y. S. Byun, T. A. Robbins, C. B. Knobler, and D. J. Cram: *J. Chem. Soc., Chem. Commun.* 1947 (1995). (l) Y. S. Byun, O. Vadhat, M. T. Blanda, C. B. Knobler, and D. J. Cram: *J. Chem. Soc., Chem. Commun.* 1825 (1995). (m) R. C. Helgeson, C. B. Knobler, and D. J. Cram: *J. Chem. Soc., Chem. Commun.* 307 (1995). (n) K. Paek, K. Joo, S. Kwon, H. Ihm, and Y. Kim: *Bull. Korean Chem. Soc.* **18**, 80 (1997). (o) K. Paek, K. Joo, and Y. Kim: *Bull. Korean Chem. Soc.* **16**, 477 (1995).
6. For tris-bridged hemicarcerands see for example: D. J. Cram, M. E. Tanner, and C. B. Knobler: *J. Am. Chem. Soc.* **113**, 7717 (1991).
  7. For asymmetric hemicarcerands see for example: (a) S. K. Kurdistani, R. C. Helgeson, and D. J. Cram: *J. Am. Chem. Soc.* **117**, 1659 (1995). (b) J. Yoon, C. Sheu, K. N. Houk, C. B. Knobler, and D. J. Cram: *J. Org. Chem.* **61**, 9323 (1996). (c) J. Yoon, C. B. Knobler, E. F. Maverick, and D. J. Cram: *J. Chem. Soc., Chem. Commun.* 1303 (1997). (d) J. Yoon and D. J. Cram: *J. Chem. Soc., Chem. Commun.* 1505 (1997). (e) E. L. Piatnitski and K. D. Deshayes: *Angew. Chem., Int. Ed. Engl.*, **37**, 970 (1998). (f) R. C. Helgeson, C. B. Knobler, and D. J. Cram: *J. Am. Chem. Soc.* **119**, 3229 (1997). (g) R. C. Helgeson, K. Paek, C. B. Knobler, E. F. Maverick, and D. J. Cram: *J. Am. Chem. Soc.* **118**, 5590 (1996). (h) P. Timmerman, W. Verboom, F. C. J. M. van Veggel, W. P. van Hoorn, and D. N. Reinhoudt: *Angew. Chem., Int. Ed. Engl.* **33**, 1292 (1994). (i) A. M. A. van Wageningen, J. P. M. van Duynhoven, W. Verboom, and D. N. Reinhoudt: *J. Chem. Soc., Chem. Commun.* 1941 (1995). (j) A. M. A. van Wageningen, P. Timmerman, J. P. M. van Duynhoven, W. Verboom, F. C. J. M. van Veggel, and D. N. Reinhoudt: *Chem. Eur. J.* **3**, 639 (1997). (k) J. R. Fraser, B. Borecka, J. Trotter, and J. C. Sherman: *J. Org. Chem.* **60**, 1207 (1995).
  8. For chiral hemicarcerands see for example: (a) J. K. Judice, and D. J. Cram: *J. Am. Chem. Soc.* **113**, 2790 (1991). (b) J. Yoon and D. J. Cram: *J. Am. Chem. Soc.* **119**, 11796 (1997). (c) B. S. Park, C. B. Knobler, C. N. Eid, Jr., R. Warmuth, and D. J. Cram: *J. Chem. Soc., Chem. Commun.* 55 (1998).
  9. For metal-assembled carcerands see for example: (a) E. Dalcanale, and P. Jacopozzi: *Angew. Chem., Int. Ed. Engl.* **36**, 613 (1997). (b) O. D. Fox, N. K. Dalley, and R. G. Harrison: *J. Am. Chem. Soc.* **120**, 7111 (1998).
  10. J. Yoon and D. J. Cram: *J. Chem. Soc., Chem. Commun.* 497 (1998).
  11. (a) R. G. Chapman, N. Chopra, E. D. Cochien, and J. C. Sherman: *J. Am. Chem. Soc.* **116**, 369 (1994). (b) R. G. Chapman and J. C. Sherman: *J. Am. Chem. Soc.* **117**, 9081 (1995). (c) R. G. Chapman and J. C. Sherman: *J. Org. Chem.* **63**, 4103 (1998). (d) R. G. Chapman, G. Olovsson, J. Trotter, and J. C. Sherman: *J. Am. Chem. Soc.* **120**, 6252 (1998). (e) R. G. Chapman and J. C. Sherman: *Tetrahedron* **53**, 15911 (1997).
  12. K. N. Houk, K. Nakamura, C. Sheu, and A. E. Keating: *Science* **273**, 627 (1996). (b) K. Nakamura and K. N. Houk: *J. Am. Chem. Soc.* **117**, 1853 (1995). (c) C. Sheu and K. N. Houk: *J. Am. Chem. Soc.* **118**, 8056 (1996).
  13. T. A. Robbins and D. J. Cram: *J. Am. Chem. Soc.* **115**, 12199 (1993).
  14. S. Mendoza, P. D. Davidov, and A. E. Kaifer: *Chem. Eur. J.* **4**, 864 (1998).
  15. A. Farrán, K. D. Deshayes, C. Matthews, and I. Balanescu: *J. Am. Chem. Soc.* **117**, 9614 (1995).
  16. A. Farrán and K. D. Deshayes: *J. Phys. Chem.* **100**, 3305 (1996).
  17. F. Pina, A. J. Parola, E. Ferreira, M. Maestri, N. Armaroli, R. Ballardini, and V. Balzani: *J. Phys. Chem.* **99**, 12701 (1995).
  18. A. J. Parola, F. Pina, E. Ferreira, M. Maestri, V. Balzani: *J. Am. Chem. Soc.* **118**, 11610 (1996).
  19. (a) M. E. Sigman, and G. L. Closs: *J. Phys. Chem.* **95**, 5012 (1991). (b) V. Balzani, M. T. Indelli, M. Maestri, D. Sandrini, and F. Scandola: *J. Phys. Chem.* **84**, 852 (1980).
  20. (a) I. Balanescu, A. Farrán, and K. D. Deshayes: *Book of Abstracts*, 231th ACS National Meeting, Part 2, ORGN 378, (1997). (b) D. W. Place, K. D. Deshayes, J. Miller, and R. Marasas Jr.: *Book of Abstracts*, 231th ACS National Meeting, Part 2, ORGN 379, (1997).

21. See for example: (a) I. R. Dunkin *Reactive Organic Species in Matrices* (Chemistry and physics of matrix-isolated species, Eds. L. Andrews, and M. Moskovits) pp. 203–237, Elsevier Science Publisher B.V. (1989). (b) M. J. Almond and A. J. Down *Spectroscopy of Matrix Isolated Species* (Advances in Spectroscopy v. 17, Eds. R. J. H. Clark and R. E. Hester) John Wiley and Sons Ltd. (1989). (c) W. Sander: *Angew. Chem., Int. Ed. Engl.* **33**, 1455 (1994). (d) A. Krebs and J. Wilke: *Top. Curr. Chem.* **109**, 189 (1983).
22. D. J. Cram, M. E. Tanner, and R. Thomas: *Angew. Chem.* **103**, 1048 (1991); *Angew. Chem., Int. Ed. Engl.* **30**, 1024 (1991).
23. (a) M. P. Cava and M. J. Mitchell: *Cyclobutadiene and Related Compounds*, Academic Press, New York (1967). (b) G. Maier: *Angew. Chem.* **100**, 317 (1988); *Angew. Chem., Int. Ed. Engl.* (1988) **27**, 309.
24. O. L. Chapman, C. L. McIntosh, and J. Pacansky: *J. Am. Chem. Soc.* 614 (1973).
25. G. Maier and A. Alzérreca: *Angew. Chem.* **85**, 1056 (1978); *Angew. Chem., Int. Ed. Engl.* **12**, 1015 (1978).
26. G. Wittig: *Naturwissenschaften* **30**, 696 (1942).
27. J. D. Roberts, H. E. Simmons, Jr., J. A. Carlsmith, and C. W. Vaughan: *J. Am. Chem. Soc.* (1953) **75**, 3290.
28. R. Warmuth: *Angew. Chem.* **109**, 1406 (1997); *Angew. Chem., Int. Ed. Engl.* **37**, 1347 (1997).
29. J. G. G. Simon, N. Münzel, and A. Schweig: *Chem Phys. Lett.* **201**, 377 (1993).
30. R. Warmuth, C. B. Knobler, and E. F. Maverick: manuscript in preparation.
31. (a) J. G. G. Simon, N. Münzel, and A. Schweig: *Chem. Phys. Lett.* **170**, 187 (1990). (b) J. G. Radziszewski, B. A. Hess Jr., and R. Zahradnik: *J. Am. Chem. Soc.* **114**, 52 (1992).
32. H. Jiao, P. von Ragué Schleyer, B. R. Beno, K. N. Houk, and R. Warmuth: *Angew. Chem.* **109**, 2710 (1997); *Angew. Chem., Int. Ed. Engl.* **37**, 2761 (1997), and references therein.
33. R. Warmuth: *J. Chem. Soc., Chem. Commun.* 59 (1998).
34. A. M. Orendt, J. C. Facelli, J. G. Radziszewski, W. J. Horton, D. M. Grant, and J. Michl: *J. Am. Chem. Soc.* **118**, 846 (1996).
35. (a) G. M. J. Schmidt: *Pure Appl. Chem.* **27**, 647 (1971). (b) J. R. Scheffer: *Acc. Chem. Res.* **13**, 283 (1980). (c) M. S. Platz: *The Chemistry, Kinetics, and Mechanisms of triplet Carbene Processes in Low-Temperature Glasses and Solids* (Kinetics and Spectroscopy of Carbenes and Biradicals, Ed. M. S. Platz) pp. 143–211, Plenum Press, New York, (1990). (d) J. M. McBride: *Acc. Chem. Res.* **16**, 304 (1983).
36. B. R. Beno, C. Sheu, K. N. Houk, R. Warmuth, and D. J. Cram: *J. Chem. Soc., Chem. Commun.* 301 (1998).
37. A. Wassermann (Ed.): *Diels-Alder Reactions* p. 44, Elsevier Publishing Comp., Amsterdam (1965).
38. H. W. Gschwend, A. O. Lee, and H. P. Meier: *J. Org. Chem.* **38**, 2169 (1973).
39. (a) H.-J. Schneider, and H. Dürr (Eds.): *Frontiers in Supramolecular Organic Chemistry and Photochemistry* VCH, Weinheim (1991). (b) V. Ramamurthy, R. G. Weiss, and G. S. Hammond: *A Model for the Influence of Organized Media on Photochemical Reactions* (Advances in Photochemistry, v. 18, Eds. D. H. Volman, G. S. Hammond, and D. C. Neckers) pp. 67–234, John Wiley & Sons (1993). (c) V. Ramamurthy, and D. F. Eaton: *Acc. Chem. Res.* **21**, 300 (1988). (d) V. Ramamurthy: (Ed.), *Photochemistry in Organized and Constrained Media* VCH, New York (1991). (e) A. Ponce, P. A. Wong, J. J. Way, and D. Nocera: *J. Phys. Chem.* **97**, 11137 (1993). (f) R. A. Bissel and A. P. de Silva: *J. Chem. Soc., Chem. Commun.* 1148 (1991). (g) V. Ramamurthy: *J. Am. Chem. Soc.* **116**, 1345 (1994), and references therein.
40. A. J. Parola, F. Pina, M. Maestri, N. Armaroli, and V. Balzani: *New J. Chem.* **18**, 659 (1994).
41. K. R. Goto and Okazaki: *Liebigs Ann./Recueil* 2393 (1997).
42. D. R. Hogg: *Chemistry of Sulphenic Acids and Esters* (The Chemistry of Sulfenic Acids and Their Derivatives, Ed. S. Patai) pp. 361–402, John Wiley & Sons, New York, (1990).

43. (a) W. S. Allison: *Acc. Chem. Res.* **9**, 293 (1976) (b) A. Claiborne, R. P. Ross, and D. Parsonage: *Trends Biochem. Sci.* **17**, 183 (1992); (c) A. Claiborne, H. Miller, D. Parsonage, and R. P. Ross: *FASEB J.* **7**, 1483 (1993).
44. The concept of concave reagents was originally developed by U. Lüning. See for example: (a) U. Lüning: *Liebigs Ann. Chem.* 949 (1987). (b) U. Lüning: *Top. Curr. Chem.* **175**, 57 (1995). (c) U. Lüning: *J. Incl. Pheno. Mol. Recognit. Chem.* **24**, 43 (1996). (d) U. Lüning: *J. Mater. Chem.* **7**, 175 (1997).
45. K. Goto, N. Tokitoh, and R. Okazaki: *Angew. Chem.* **107**, 1202 (1995); *Angew. Chem., Int. Ed. Engl.* **34**, 1124 (1995).
46. (a) T. Saiki, K. Goto, N. Tokitoh, and R. Okazaki: *J. Org. Chem.* **61**, 2924 (1996). (b) T. Saiki, K. Goto, N. Tokitoh, M. Goto, and R. Okazaki: *Tetrahedron Lett.* **37**, 4039 (1996). (c) T. Saiki, K. Goto, R. Okazaki: *Chem. Lett.* 993 (1996). (d) T. Saiki, K. Goto, and R. Okazaki: *Angew. Chem.* **109**, 2320 (1997); *Angew. Chem., Int. Ed. Engl.* **36**, 2223 (1997).
47. K. Goto, M. Holler, and R. Okazaki: *Tetrahedron Lett.* **37**, 3141 (1996).
48. K. Goto, M. Holler, and R. Okazaki: *J. Am. Chem. Soc.* **119**, 1460 (1997).
49. K. Goto, M. Holler, and R. Okazaki: *J. Chem. Soc., Chem. Commun.* 1915 (1998).
50. S. Watanabe, K. Goto, T. Kawashima, and R. Okazaki: *Tetrahedron Lett.* **36**, 7677 (1995).
51. S. Watanabe, K. Goto, T. Kawashima, and R. Okazaki: *J. Am. Chem. Soc.* **119**, 3195 (1997).
52. For recent review articles see for example: (a) J. de Mendoza: *Chem. Eur. J.* **4**, 1373 (1998). (b) M. M. Conn and J. Rebek Jr.: *Chem. Rev.* **97**, 1647 (1997). (c) J. Rebek Jr.: *Chem. Soc. Rev.* **25**, 255 (1996). (d) J. Rebek Jr.: *Pure Appl. Chem.* **68**, 1261 (1996).
53. For selected self-assembled containers see: (a) R. Wyler, J. de Mendoza, and J. Rebek Jr.: *Angew. Chem., Int. Ed. Engl.* **32**, 1699 (1993). (b) T. Martin, U. Obst, and J. Rebek Jr.: *Science* **281**, 1842 (1998). (c) S. H. Ma, D. M. Rudkevich, and J. Rebek Jr.: *J. Am. Chem. Soc.* **120**, 4977 (1998). (d) J. M. Rivera, T. Martin, and J. Rebek Jr.: *Science* **279**, 1021 (1998). (e) Y. Tokunaga and J. Rebek Jr.: *J. Am. Chem. Soc.* **120**, 66 (1998). (f) R. K. Castellano, B. H. Kim, and J. Rebek Jr.: *J. Am. Chem. Soc.* **119**, 12671 (1997). (g) Y. Tokunaga, D. M. Rudkevich, and J. Rebek Jr.: *Angew. Chem., Int. Ed. Engl.* **36**, 2656 (1997). (h) B. M. O'Leavy, R. M. Grotzfeld, and J. Rebek Jr.: *J. Am. Chem. Soc.* **119**, 11701 (1997). (i) R. Meissner, X. Garcias, S. Mecozzi, J. Rebek Jr.: *J. Am. Chem. Soc.* **119**, 77 (1997). (j) B. C. Hamann, K. D. Shimizu, and J. Rebek Jr.: *Angew. Chem., Int. Ed. Engl.* **35**, 1326 (1996). (k) R. M. Grotzfeld, N. Branda, and J. Rebek Jr.: *Science*, **271**, 487 (1996). (l) K. D. Shimizu and J. Rebek Jr.: *Proc. Natl. Acad. Sci USA* **92**, 12403 (1995). (m) R. Meissner, J. Rebek Jr., J. de Mendoza: *Science* **270**, 1485 (1995). (n) J. Kang, and J. Rebek Jr.: *Nature* **382**, 239 (1996). (o) O. Mogck, E. F. Paulus, V. Boehmer, I. Thondorf, and W. Vogt: *J. Chem. Soc., Chem. Commun.* 2533 (1996). (p) O. Mogck, M. Pons, V. Boehmer, I. Thondorf, and W. Vogt: *Tetrahedron Lett.* **52**, 8489 (1996). (q) O. Mogck, E. F. Paulus, V. Boehmer, and W. Vogt: *J. Am. Chem. Soc.* **119**, 5706 (1997). (r) R. G. Chapman and J. C. Sherman: *J. Am. Chem. Soc.* **117**, 9081 (1995). (s) R. G. Chapman, G. Olovsson, J. Trotter, and J. C. Sherman: *J. Am. Chem. Soc.* **120**, 6252 (1998).
54. Y. Tokunaga, D. M. Rudkevich, J. Santamaría, G. Hilmersson, and J. Rebek Jr.: *Chem. Eur. J.* **4**, 1449 (1998).
55. J. Kang, J. Santamaría, G. Hilmersson, and J. Rebek Jr.: *J. Am. Chem. Soc.* **120**, 7389 (1998). (b) J. Kang, G. Hilmersson, J. Santamaría, and J. Rebek Jr.: *J. Am. Chem. Soc.* **120**, 3650 (1998). (c) J. Kang and J. Rebek Jr.: *Nature* **385**, 50 (1996).
56. D. Hilvert, K. W. Hill, and M. T. M. Auditor: *J. Am. Chem. Soc.* **111**, 9261 (1989).
57. (a) H. W. Kroto, J. R. Heath, S. C. O'Brien, R. F. Curl, and R. E. Smalley: *Nature* **318**, 162 (1985). (b) W. Krätschmer, L. D. Lamb, K. Fostiropoulos, and D. R. Huffman: *Nature* **347**, 354 (1990).
58. (a) D. S. Bethune, R. D. Johnson, J. R. Salem, M. S. de Vries, and C. S. Yannoni: *Nature* **366**, 123 (1993). (b) F. T. Edelman: *Angew. Chem., Int. Ed. Engl.* **34**, 981 (1995). (c) R. Tellgmann, N. Krawez, S.-H. Lin, I. V. Hertel, and E. E. B. Campbell: *Nature* **382**, 407 (1996).

59. (a) T. Weiske, D. K. Böhme, J. Hrusák, W. Krätschmer, and H. Schwarz: *Angew. Chem.* **103**, 898 (1991); *Angew. Chem., Int. Ed. Engl.* **30**, 884 (1991). (b) T. Weiske, J. Hrusák, D. K. Böhme, and H. Schwarz: *Chem. Phys. Lett.* **186**, 459 (1991). (c) T. Weiske, D. K. Böhme, and H. Schwarz: *J. Phys. Chem.* **95**, 8451 (1991). (d) T. Weiske, T. Wong, W. Krätschmer, J. K. Terlou, and H. Schwarz: *Angew. Chem.* **104**, 242 (1992); *Angew. Chem., Int. Ed. Engl.* **31**, 183 (1992). (e) M. Saunders, H. A. Jiménez-Vázquez, R. Shimshi, and A. Kkong: *Science* **271**, 1693 (1996). (f) M. Rüttimann, R. F. Haldimann, L. Isaacs, F. Diederich, A. Kkong, H. A. Jiménez-Vázquez, R. J. Cross, and M. Saunders: *Chem. Eur. J.* **3**, 1071 (1997).
60. (a) A. F. Hedard, M. J. Rosseinsky, R. C. Haddon, D. W. Murphy, S. H. Glarum, T. T. M. Palstra, A. P. Ramirez, and A. R. Kortan: *Nature* **350**, 600 (1991). (b) K. Holczer, O. Klein, S. M. Huang, R. B. Kaner, K. J. Fu, R. L. Whetten, and F. Diederich: *Science* **252**, 1154 (1991).
61. P. M. Allemand, K. C. Khemani, A. Koch, F. Wudl, K. Holzer, S. Donovan, G. Grüner, and J. D. Thompson: *Science* **253**, 301 (1991).
62. Nalwa H. S. *Adv. Mater.* **5**, 341–358 (1993).
63. (a) T. Almeida Murphy, T. Pawlik, A. Weidinger, M. Höhne, R. Alcalá, and J.-M. Spaeth: *Phys. Rev. Lett.* **77**, 1075 (1996). (b) C. Knapp, K.-P. Dinse, B. Pietzak, M. Waiblinger, and A. Weidinger: *Chem. Phys. Lett.* **272**, 433 (1997).
64. H. Mauser, N. J. R. van Eikema Hommes, T. Clark, A. Hirsch, B. Pietzak, A. Weidinger, and L. Dunsch: *Angew. Chem. Int. Ed. Engl.* **37**, 2835 (1997).
65. (a) A. Hirsch: *The Chemistry of the Fullerenes*, Thieme, Stuttgart (1994). (b) Haddon R. C. *Science* **261**, 1545 (1993).
66. R. C. Haddon: *Acc. Chem. Res.* **25**, 127 (1992).
67. S. Patchkovskii and Thiel W. *J. Am. Chem. Soc.* **118**, 7164 (1996).
68. Y. Rubin *Chem. Eur. J.* **3**, 1009 (1997), and references therein.



**Ralf Warmuth** was born in Germany. He studied chemistry at the University of Cologne, Germany and received his Diploma in biochemistry (1989) under the guidance of Professor Ernst Bause. He carried out his thesis work at the Max-Planck Institute for Biophysics in Frankfurt/M., Germany and at the Institute Le Bel of the Université Louis Pasteur in Strasbourg, France with Dr. Ernst Grell, Professor Jean-Marie Lehn and Professor Gerhard Quinkert as his advisors and obtained his Ph.D. from the Johann Wolfgang Goethe-University at Frankfurt/M., in 1992. After postdoctoral work with Dr. Mark Mascal at the University of Nottingham, U.K. (1992–1994) and with professor Donald J. Cram and Professor Ken

N. Houk at the University of California, Los Angeles (1994–1997, Feodor Lynen fellow), he joined Kansas State University as an Assistant Professor in 1997. His research focuses on inner phase chemistry, protein structure and protein folding.